Effective field theory for vibrations in odd-mass nuclei

E. A. Coello Pérez[1,2,3] and T. Papenbrock[3,4]
[1]*Institut für Kernphysik, Technische Universität Darmstadt, 64289 Darmstadt, Germany*
[2]*ExtreMe Matter Institute EMMI, Helmholtzzentrum für Schwerionenforschung GmbH, 64291 Darmstadt, Germany*
[3]*Department of Physics and Astronomy, University of Tennessee, Knoxville, Tennessee 37996, USA*
[4]*Physics Division, Oak Ridge National Laboratory, Oak Ridge, Tennessee 37831, USA*
(Received 10 August 2016; published 17 November 2016)

Heavy even-even nuclei exhibit low-energy collective excitations that are separated in scale from the microscopic (fermion) degrees of freedom. This separation of scale allows us to approach nuclear vibrations within an effective field theory (EFT). In odd-mass nuclei collective and single-particle properties compete at low energies, and this makes their description more challenging. In this article we describe spherical odd-mass nuclei with ground-state spin $I = \frac{1}{2}$ by means of an EFT that couples a fermion to the collective degrees of freedom of an even-even core. The EFT relates observables such as energy levels, electric quadrupole transition strengths, and magnetic dipole moments of the odd-mass nucleus to those of its even-even neighbor and allows us to quantify theoretical uncertainties. For isotopes of rhodium and silver the theoretical description is consistent with data within experimental and theoretical uncertainties. Several testable predictions are made.

DOI: 10.1103/PhysRevC.94.054316

I. INTRODUCTION

Collective modes such as rotations and vibrations are often the lowest-lying excitations in heavy nuclei [1], and these phenomena can be understood in terms of collective models [2–9] of the atomic nucleus. In odd-mass nuclei, collective excitations compete with single-particle excitations already at low energies. The well-known particle-rotor, particle-vibrator, and boson-fermion models couple the odd fermion to the collective (boson) degrees of freedom [10–22]. While these models successfully describe various aspects of odd-mass nuclei, it is difficult to systematically improve them or to give theoretical uncertainties for the computed results.

In this paper, we want to reexamine odd-mass nuclei within an EFT that couples a fermionic degree of freedom to the bosonic degrees of freedom of the even-even nucleus. EFTs provide us with systematically improvable approaches to nuclear interactions [23–27], clustering in nuclei [28–30], nuclear rotations [31–35], and vibrations [36]. They also allow us to quantify theoretical uncertainties [37–40]. This is an advantage over traditional models. EFTs also allow us to derive relations between observables (as opposed to relations between model parameters and observables), and this makes their application interesting even in cases where microscopic approaches to nuclear collective phenomena are available [41–47].

Because EFTs are based on a separation of scales, we remind the reader about the relevant low-energy scales in heavy nuclei. In heavy deformed even-even nuclei, rotational excitations (at about 0.1 MeV or less) are separated in scale from vibrations (at about 0.8 MeV), which in turn are separated from fermion excitations such as pair breaking (at about 2–3 MeV). In heavy spherical even-even nuclei, vibrations (at an energy $\omega \approx 0.6$ MeV) are lowest in energy and separated from fermion excitations such as pair breaking at about $\Lambda \approx 2$–3 MeV. In the recently proposed boson EFT for nuclear vibrations in spherical nuclei [36], the fermion energy scale is the breakdown scale, and the "small" expansion parameter is $\omega/\Lambda \approx \frac{1}{3}$.

In this work we construct an EFT for spherical odd-mass nuclei with spin $\frac{1}{2}$ in their ground states by coupling an odd nucleon in a $j = \frac{1}{2}$ orbital to the quadrupole degrees of freedom that govern the collective vibrations of an even-even nucleus. This EFT is based on the usual linear Wigner–Weyl representation of rotational symmetry and can be contrasted to an EFT for deformed nuclei, which is based on the nonlinear Nambu–Goldstone realization of the rotational symmetry [31]. Based on a power counting we systematically construct the Hamiltonian and electromagnetic operators. Another interesting aspect of this EFT approach is the simultaneous description of the even-even and neighboring odd-mass nuclei; consequently, observables in the even-even nucleus are related to observables in the odd-mass system. These relations can be confronted with experimental data. In this work, we compute electric quadrupole $E2$ and magnetic dipole $M1$ observables for odd-mass isotopes of rhodium and silver. This is also interesting in view of recent g-factor measurements in this region of the nuclear chart [48,49]. The paper is organized as follows: In Sec. II, we present the EFT framework within which the even-even/odd-mass nuclei will be described, establish a power counting and describe energy spectra at next-to-next-to-leading order (NNLO). Sections III and IV are dedicated to the study of moments and transitions of the $E2$ and $M1$ operators, respectively. In Sec. V we discuss the possible extension of the EFT to the more complicated case posed by cadmium isotopes. Finally, in Sec. VI we present our summary.

II. ODD-MASS VIBRATIONAL NUCLEI

Certain even-even nuclei (such as isotopes of Cd, Ru, and Te) exhibit low-energy states that resemble those of a five-dimensional quadrupole oscillator. In these nuclei, the vibrational frequency $\omega \approx 0.6$ MeV is the energy scale of interest, and the picture of a quadrupole vibrator breaks down at an energy $\Lambda \approx 2$–3 MeV, i.e., around the three-phonon

level. The breakdown scale Λ is associated with neglected microscopic (fermionic) degrees of freedom and is of similar size as the pairing gap. Thus, $\omega \ll \Lambda$ holds, and this separation of scale has been exploited in Ref. [36] to construct an EFT for nuclear vibrations.

The spectra of certain odd-mass neighbors of vibrational nuclei are relatively simple and suggest that these result from coupling a $j^\pi = \frac{1}{2}^-$ fermion to the even-even nucleus. Examples we consider in this paper are ^{99,101,103}Rh ($Z = 45$) and ^{105,107,109,111}Ag ($Z = 47$) as a proton coupled to ^{98,100,102}Ru ($Z = 44$) and ^{104,106,108,110}Pd ($Z = 46$), respectively, or ^{107,109,111}Ag as a proton-hole in ^{108,110,112}Cd ($Z = 48$). These cases are particularly simple because one deals with a $j^\pi = \frac{1}{2}^-$ degree of freedom. We note here that the odd-mass nuclei considered in this work also exhibit very-low-lying (100 keV or less) states with positive parity. Because a single fermion cannot undergo parity-changing transitions, the positive-parity states can be neglected in the description of low-lying negative-parity states in the odd-mass nuclei.

Could one also attempt to describe, for instance, ^{108,110,112}Cd in terms of two protons added to ^{106,108,110}Pd, respectively? In such an EFT approach, the low-lying positive-parity states of ^{107,109,111}Ag would also need to enter the description. The calculation would be nonperturbative (because of the near degeneracy of states with positive and negative parities in the odd-mass nucleus), and a significant number of fermionic two-body-matrix elements would enter as low-energy constants (LECs). It is thus unclear whether such an EFT approach would be profitable.

A. Hamiltonian

Before we turn to the odd-mass nuclei, we briefly review some aspects of the EFT for nuclear vibrations in even-even nuclei [36]. The relevant degrees of freedom are quadrupole operators $d_\mu^\dagger$ and d_μ with $\mu = -2, -1, \ldots, 2$ that create and annihilate a phonon, respectively. They fulfill the usual boson commutation relations

$$[d_\mu, d_\nu^\dagger] = \delta_{\mu\nu}. \tag{1}$$

We note that $d_\mu^\dagger$ and

$$\tilde{d}_\mu = (-1)^\mu d_{-\mu} \tag{2}$$

are spherical tensors of rank two. The angular-momentum operator for the quadrupole degrees of freedom is the vector

$$\hat{\mathbf{J}} = \sqrt{10}(d^\dagger \otimes \tilde{d})^{(1)}. \tag{3}$$

We recall that the coupling of the spherical tensors $\mathcal{M}^{(m)}$ and $\mathcal{N}^{(n)}$ of ranks m and n, respectively, to a spherical tensor $\mathcal{K}^{(k)}$ of rank k is denoted as

$$\mathcal{K}^{(k)} = (\mathcal{M}^{(m)} \otimes \mathcal{N}^{(n)})^{(k)}, \tag{4}$$

and the corresponding components

$$\mathcal{K}_\kappa^{(k)} = \sum_{\mu\nu} C_{m\mu n\nu}^{k\kappa} \mathcal{M}_\mu^{(m)} \mathcal{N}_\nu^{(n)} \tag{5}$$

are given in terms of the Clebsch–Gordan coefficients $C_{m\mu n\nu}^{k\kappa}$ that couple the angular momenta m and n to spin k [50]. Similarly, the scalar product of two spherical tensors $\mathcal{M}^{(I)}$ and $\mathcal{N}^{(I)}$ of the same rank I is [50]

$$\mathcal{M}^{(I)} \cdot \mathcal{N}^{(I)} = \sqrt{2I+1}(\mathcal{M}^{(I)} \otimes \mathcal{N}^{(I)})^{(0)}. \tag{6}$$

The boson Hamiltonian at next-to-leading order (NLO) in the EFT for vibrational nuclei is

$$\hat{H}_\mathrm{b} = \omega_1 \hat{N} + g_N \hat{N}^2 + g_v \hat{\Lambda}^2 + g_J \hat{J}^2. \tag{7}$$

Here,

$$\hat{N} \equiv d^\dagger \cdot \tilde{d} \tag{8}$$

and

$$\hat{\Lambda}^2 \equiv -(d^\dagger \cdot d^\dagger)(\tilde{d} \cdot \tilde{d}) + \hat{N}^2 - 3\hat{N} \tag{9}$$

are the boson number operator and the second-order Casimir operator, respectively. For more details on the latter operator and its eigenvalues see, for example, Ref. [9]. The first term on the right-hand side of Eq. (7) is of order ω. This leading-order (LO) term is the Hamiltonian of a five-dimensional harmonic oscillator. The remaining terms in the Hamiltonian (7) account for finer details at order ω^3/Λ^2. These corrections introduce anharmonicities. The power counting of the EFT is in powers of the small parameter ω/Λ. For details, we refer the reader to Ref. [36].

The spin-$\frac{1}{2}$ fermion is described in terms of fermion creation and annihilation operators $a_\nu^\dagger$ and a_ν, respectively, that fulfill the usual anticommutation relations

$$\{a_\mu, a_\nu^\dagger\} = \delta_{\mu\nu}. \tag{10}$$

In most of this paper, $\nu = -\frac{1}{2}, \frac{1}{2}$. The corresponding angular-momentum operator is

$$\hat{\mathbf{j}} = \frac{1}{\sqrt{2}}(a^\dagger \otimes \tilde{a})^{(1)}, \tag{11}$$

and the fermion number operator is

$$\hat{n} \equiv a^\dagger \cdot \tilde{a}. \tag{12}$$

Here, we used the spherical rank-$\frac{1}{2}$ tensor $\tilde{a}$ with components

$$\tilde{a}_\nu \equiv (-1)^{j+\nu} a_{-\nu}. \tag{13}$$

The fermion Hamiltonian

$$\hat{H}_\mathrm{f} = -S\hat{n} - \Delta\hat{n}(\hat{n} - 1) \tag{14}$$

consists of a one-body term and a two-body term. We note that the term $\hat{n}(\hat{n} - 1)$ is the unique two-body interaction for spin-$\frac{1}{2}$ fermions restricted to a single $j^\pi = \frac{1}{2}^+$ shell. We do not need to consider other Hamiltonian terms such as $\hat{j}^2 \propto \hat{n}(2 - \hat{n})$ or $\hat{n}^2$ because these are linear combinations of the terms already included in the Hamiltonian (14).

The Hamiltonian (14) is not the Hamiltonian of free fermions but rather captures the interactions between fermions and the ground state of the vibrating core. Let us discuss the energy scales S and Δ. For a particle (hole) added to the even-even vibrator, $S \approx 8$ MeV ($S \approx -8$ MeV) is of the order of the separation energy, while $\Delta \approx 2$ MeV is of the order of a paring gap. The attractive interaction between two nucleons (with isospin one) fail to bind the pair in vacuum but yields

a bound state with energy Δ when coupled to the core. We note that $\Delta \sim \Lambda$, because pairing effects are one source for the breakdown of the EFT in even-even nuclei.

Besides the breaking of a pair, there are other effects that lead to the breakdown of the EFT. In the EFT presented in this work we considered the simplest case of a single orbital with spin $\frac{1}{2}$, and in the nuclei we describe this orbital has negative parity. A view of nuclear data tables shows that there are many more states in odd-mass nuclei than predicted by our EFT. Additional negative-parity states appear at about the two-phonon level, and their omission is therefore consistent with our breakdown scale. Such states could presumably be included by adding other negative-parity orbitals to our EFT, but we did not attempt this. However, positive-parity states can be found at very low energies. As the strong nuclear interaction preserves parity, such orbitals cannot be coupled to the negative-parity orbital we consider in our EFT for a single nucleon added to the vibrating core. Thus, the description of negative-parity states below the breakdown scale is not affected by the omission of any other orbitals. We did not attempt to develop an EFT for the positive-parity states because the spin of the corresponding orbitals is rather large for the nuclei we consider. The coupling of such an orbital to the vibrating core yields a large number of possible fermion states, and it is not clear how to identify such states unambiguously. It is clear that an extension of the EFT to describe, for instance, pair transfer between even-even vibrating nuclei would be considerably more complicated because low-lying positive parity states would also need to be included.

The interaction between boson and fermion degrees of freedom is most interesting. Two-body terms of the structure $\hat{\mathbf{J}} \cdot \hat{\mathbf{j}}$ and $\hat{N}\hat{n}$ couple phonons to fermions. Here, the first term could be referred to as a "Coriolis" interaction, because it couples the spin of the fermion to the spin of the core. In addition to these interactions there are three-body terms of the form $\hat{N}^2\hat{n}$, $\hat{J}^2\hat{n}$, and $\hat{N}\hat{n}(\hat{n}-1)$. Here, the first two three-body terms involve the annihilation and creation of two phonons and are suppressed in comparison to the three-body term involving only one phonon. Thus, the leading-order interactions between phonons and fermion degrees of freedom are

$$H_{\text{b-f}} = g_{Jj}\hat{\mathbf{J}} \cdot \hat{\mathbf{j}} + \omega_2 \hat{N}\hat{n} + \omega_3 \hat{N}\hat{n}(\hat{n}-1). \tag{15}$$

We note that the three-body term $\omega_3 \hat{N}\hat{n}(\hat{n}-1)$ is only active when two fermions are coupled to the vibrating core.

Let us attempt to establish a power counting for operators involving fermion degrees of freedom. For an operator $\hat{O}_n$ consisting of $2n$ fermion annihilation and creation operators, we propose its matrix elements to scale as

$$\langle \hat{O}_n \rangle \sim \langle \hat{O}_{n-1} \rangle \frac{\omega}{\Lambda}. \tag{16}$$

This scaling is based on the relatively small energy difference observed between the two different levels that result from coupling a fermion to the one-phonon state of the even-even nucleus and consistent with the shift of the centroid of these two levels in the odd-mass nucleus. We note that the energy splitting and the shift of the centroid is due to the first and second terms in the interaction Hamiltonian (15), respectively. Comparing these energies with that of the one-phonon state in the even-even neighbor, given by the matrix element of the LO term in the boson Hamiltonian (7), leads to the power counting proposed in Eq. (16). Thus, one-fermion terms in the interaction Hamiltonian (15) scale as ω^2/Λ.

Putting everything together, and restricting ourselves to a single fermion, we arrive at the Hamiltonian

$$\begin{aligned} H &= H_{\text{b}} + H_{\text{f}} + H_{\text{b-f}} \\ &= -S\hat{n} + H_{\text{LO}} + H_{\text{NLO}} + H_{\text{NNLO}}, \end{aligned} \tag{17}$$

with

$$H_{\text{LO}} \equiv \omega_1 \hat{N}, \tag{18}$$

$$H_{\text{NLO}} \equiv g_{Jj}\hat{\mathbf{J}} \cdot \hat{\mathbf{j}} + \omega_2 \hat{N}\hat{n}, \tag{19}$$

and

$$H_{\text{NNLO}} \equiv g_N \hat{N}^2 + g_v \hat{\Lambda}^2 + g_J \hat{J}^2. \tag{20}$$

While the term $-S\hat{n}$ in Eq. (17) sets the overall binding with respect to the ground-state of the vibrating core, it does not contain any spectroscopic information. We will therefore neglect this term in what follows. The LO Hamiltonian (18) is that of a harmonic quadrupole vibrator, and energies are of the order ω. Higher-order contributions to the Hamiltonian are most interesting. The NLO Hamiltonian (19) accounts for effects introduced by the phonon-fermion couplings. We note that the size of the boson-fermion interaction cannot be determined on theoretical grounds but must rather be based on data. The empirical inspection of spectra suggests that these phonon-fermion couplings are a fraction of the scale ω. We approximate this scale as order ω^2/Λ and thereby avoid the introduction of a new small parameter. Because of this perturbative coupling we can associate low-lying states in certain odd-mass nuclei with the spectra in the neighboring even-even nuclei. The NNLO Hamiltonian (20) involves phonon-phonon interactions that account for anharmonicities in the even-even nucleus. We remind the reader that these terms are of order ω^3/Λ^2 and have been discussed in detail in Ref. [36].

Let us discuss the Hilbert space. The states of the odd nucleus are products of the boson quadrupole states and fermion states of the $j = \frac{1}{2}$ orbital. As usual, the vacuum $|0\rangle$ fulfills

$$d_\mu|0\rangle = 0 = a_\nu|0\rangle. \tag{21}$$

The boson states of the quadrupole vibrator are created from the vacuum by the successive application of quadrupole creation operators. These states are denoted

$$|N\alpha v J\mu\rangle. \tag{22}$$

Here, N is the number of phonons, v is the seniority, J and μ are the angular momentum and its projection onto the z axis, respectively, while α represents an additional quantum number. This quantum number is only needed above the two-phonon level and therefore is not needed for the low-energy physics in which we are interested. We will omit it in what follows. For details on the construction of these states we refer the reader to Ref. [9]. The single-fermion states are

$$\left|\tfrac{1}{2}\nu\right\rangle \equiv a_\nu^\dagger|0\rangle. \tag{23}$$

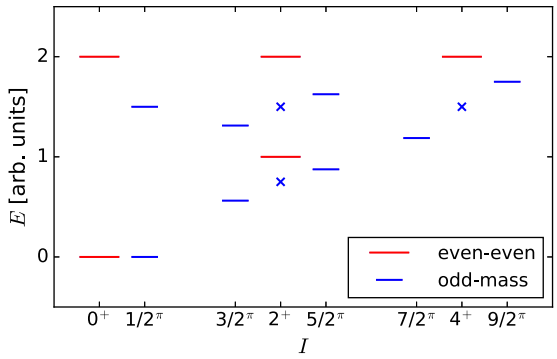

FIG. 1. NLO spectrum for the fermion in a $j = \frac{1}{2}$ orbital coupled to a quadrupole vibrator up to the two-phonon level in arbitrary units. The states labeled I^π are displayed as long red and short blue lines for even-even and odd-mass nuclei, respectively. The centroids of the $I = J \pm j$ odd-mass states are shown as blue crosses.

Normalized states of the odd-mass nucleus with total spin I and projection M are

$$\left|IM; N\alpha vJ; \tfrac{1}{2}\right\rangle \equiv \left(|N\alpha vJ\rangle \otimes \left|\tfrac{1}{2}\right\rangle\right)^{(I)}_{M} = \sum_{\mu\nu} C^{IM}_{J\mu\frac{1}{2}\nu} |N\alpha vJ\mu\rangle \left|\tfrac{1}{2}\nu\right\rangle. \quad (24)$$

The Hamiltonian (17) is diagonal in the basis states (24) with eigenvalues

$$E = E_{\mathrm{LO}} + E_{\mathrm{NLO}} + E_{\mathrm{NNLO}}, \quad (25)$$

with

$$E_{\mathrm{LO}} = \omega_1 N, \quad (26)$$

$$E_{\mathrm{NLO}} = \omega_2 N n + \frac{g_{Jj}}{2}\left[I(I+1) - J(J+1) - \frac{3}{4}\right], \quad (27)$$

and

$$E_{\mathrm{NNLO}} = g_N N^2 + g_v v(v+3) + g_J J(J+1). \quad (28)$$

We remind the reader that we neglected the separation energy S, i.e., the ground-state energies of the even-even nucleus and of the odd-mass nucleus are set to zero. Figure 1 shows a schematic plot of the NLO energy spectrum (25) up to the two-phonon level. States are labeled by their spin and parity. Even-even states, shown as long red lines, have integer spins and positive parity. Odd-mass states, shown as short blue lines, have half-integer spins and the parity of the fermion's orbital. (Odd-mass states considered in what follows all have negative parities.) Energies are chosen in units of ω_1, and the LECs ω_2 and g_{Jj} are small fractions of this LEC. We see how the term proportional to ω_2 shifts the energies while the term proportional to g_{Jj} splits even-even states with finite spins into doublets in the odd-mass neighbor. The centroids from the shift are shown as crosses in Fig. 1.

B. Uncertainty quantification

EFTs provide us with the opportunity to quantify theoretical uncertainties. While the power counting allows one to estimate uncertainties in EFTs, quantified uncertainties result from (testable) assumptions one makes about the distribution of the LECs [40] in form of priors. Employing Bayesian statistics (and marginalizing) over unknown parameters included in these priors yields degree-of-belief (DOB) intervals with a statistical meaning. In this section, we closely follow Ref. [36] and chose log-normal priors for the LECs' distribution functions.

The energies of the states below the breakdown scale can be written as an expansion of the form

$$E(I^\pi) = \omega_1 \sum_i^\infty c_i(I^\pi)\varepsilon^i, \quad (29)$$

with

$$\varepsilon \equiv N\frac{\omega_1}{\Lambda}. \quad (30)$$

In our case

$$\frac{\omega_1}{\Lambda} \approx \frac{1}{3}. \quad (31)$$

If the expansion is truncated at order $O(\varepsilon^2)$, a comparison with the NNLO spectrum (25) allows us to identify

$$c_0(I^\pi) \equiv \frac{E_{\mathrm{LO}}(I^\pi)}{\omega_1}, \quad (32)$$

$$c_1(I^\pi) \equiv \frac{E_{\mathrm{NLO}}(I^\pi)}{\varepsilon\omega_1}, \quad (33)$$

$$c_2(I^\pi) \equiv \frac{E_{\mathrm{NNLO}}(I^\pi)}{\varepsilon^2\omega_1}. \quad (34)$$

From the power counting one expects these coefficients to be of order $O(1)$.

Figure 2 shows the cumulative distributions of the c_1 and c_2 coefficients for the energies of states below the breakdown scale in an ensemble containing the data of all studied Pd and Ag nuclei. These distributions, with means μ_1 and μ_2, respectively, can be approximated by the Gaussian prior

$$\mathrm{pr}^{(\mathrm{G})}(\tilde{c}_i|c) = \frac{1}{\sqrt{2\pi}sc}\exp\left(-\frac{\tilde{c}_i^2}{2s^2c^2}\right), \quad \text{with } s = \frac{2}{3}, \quad (35)$$

for the expansion coefficient $c_i = \tilde{c}_i + \mu_i$. Here, $\mu_i \equiv \overline{c_i}$ is the mean value of c_i. The parameter c, associated with the width of the distribution, is not taken from Fig. 2. Instead, we make the assumption that c is log-normal distributed according to

$$\mathrm{pr}(c) = \frac{1}{\sqrt{2\pi}\sigma c}e^{-\frac{\log^2 c}{2\sigma^2}}. \quad (36)$$

The log-normal distribution is consistent with the EFT expectation that LECs are of natural size, i.e., that the coefficient c is of order one [37]. Given the priors (35) and (36), one calculates the probability distribution function (PDF) for c_i by marginalizing over the parameter c and finds

$$p(c_i - \mu) = \int_0^\infty dc\,\mathrm{pr}^{(\mathrm{G})}(c_i - \mu_i|c)\mathrm{pr}(c). \quad (37)$$

The cumulative distribution for c_i, denoted $\mathrm{CDF}(c_i)$, is then given in terms of the PDF (37) by

$$\mathrm{CDF}(c_i) = \int_{-\infty}^{c_i} dx\,p(x - \mu_i). \quad (38)$$

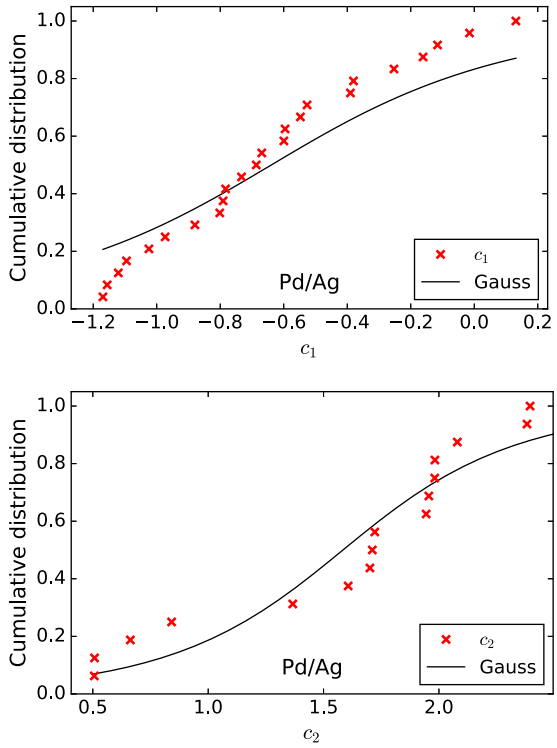

FIG. 2. Cumulative distributions of the c_1 (top) and c_2 (bottom) coefficients for the energies of states below breakdown in an ensemble containing the data of all studied Pd and Ag nuclei. These distributions, centered at μ_1 and μ_2, are approximated by Gaussian priors (shown as lines).

Bayesian methods can be employed to quantify the uncertainties associated with the energies [37,40] at any order. From the EFT expansion for an observable

$$X = X_0 \sum_i^{\infty} c_i \varepsilon^i, \tag{39}$$

it is clear that an order-k calculation has a normalized uncertainty that can be approximately written as

$$\Delta^{(k)} = \sum_{i=k+1}^{k+M} c_i \varepsilon^i. \tag{40}$$

The PDF for the normalized uncertainty can be calculated from the priors for the expansion coefficients (35) and the width parameter (36) via Bayesian methods. We employed the expressions given in Ref. [36] to calculate the PDF for the normalized uncertainty given the known coefficients, denoted by $p(\Delta|c_0,\ldots,c_k)$, within the next-term approximation; that is, setting $M = 1$.

Given $p(\Delta|c_0,\ldots,c_k)$, the DOB of the interval $[\alpha,\beta]$ is defined by

$$\mathrm{DOB}(\alpha,\beta) = \int_\alpha^\beta d\Delta p(\Delta|c_0,\ldots,c_k). \tag{41}$$

We employ an interval of the form $[-\delta,\delta]$ with $\mathrm{DOB}(-\delta,\delta) = 0.68$ to quantify the uncertainty $\Delta X^{(k)}$ associated with the order-k calculation for X as

$$\Delta X^{(k)} \equiv X_0 \delta. \tag{42}$$

Statistically, one expects 68% of the experimental data to fall within the theoretical uncertainty quantified by this DOB interval, chosen in analogy to "one-sigma" deviations.

C. Spectra

We need to adjust the LECs of our EFT to data from an even-even and an odd-mass nucleus simultaneously. The spectra of such an even-even/odd-mass system must resemble Eq. (25), schematically shown in Fig. 1. We recall that the EFT does not distinguish between a fermion particle or a fermion hole. This allows us to describe the isotopes ^{107,109,111}Ag as a proton coupled to ^{106,108,110}Pd or as a proton hole coupled to ^{108,110,112}Cd. Assuming the validity of our EFT approach, both descriptions should agree within theoretical uncertainties.

Table I lists the LECs for the systems studied in this work. Odd-mass nuclei in these systems have $I^\pi = \frac{1}{2}^-$ ground states. The LECs were fit by employing data for the energies of states identified as one- or two-phonon levels. Most of the states employed in the fit have definite assignments of spins and parities. For states with tentative spins, we made the following assignments: $I^\pi = \frac{3}{2}^-$ for the state at 410.9 keV in ^{99}Rh; $I^\pi = \frac{3}{2}^-$ and $I^\pi = \frac{7}{2}^-$ for the states at 305.4 and 851.3 keV in ^{101}Rh, respectively; $I^\pi = \frac{7}{2}^-$ for the state at 973.3 keV in ^{107}Ag. These assignments were based on the decay patterns from these states to other phonon states and they agree with tentative spin assignments. The data were taken from Refs. [51–65].

Figures 3–5 show the NNLO energy spectra of the systems listed in Table I. In these figures, even-even and odd-mass states are shown on the left and right sides, respectively. States employed to fit the LECs are shown as thick black lines, while additional states with a definitely known spin-parity assignment or a single tentative spin-parity assignment are shown as thin black lines. Observed levels with more than one tentative spin-parity assignment are not shown in these figures, and we limited ourselves to negative-parity states in the odd-mass nuclei. The NNLO energies (25) for the even-even and odd-mass nuclei are shown as red crosses. Uncertainties associated with these energies are shown as red shaded areas.

TABLE I. LECs in keV employed to generate the NNLO spectra of selected even-even/odd-mass systems studied in this work.

System	ω_1	ω_2	g_{Jj}	g_N	g_v	g_J
^{98}Ru /^{99}Rh	570.4	−231.3	6.8	45.3	9.3	− 0.1
^{100}Ru /^{101}Rh	376.6	−204.0	19.9	94.3	27.2	− 6.7
^{102}Ru /^{103}Rh	341.3	−141.9	24.9	83.2	9.3	2.2
^{104}Pd /^{105}Ag	439.3	−157.1	34.5	115.8	− 8.9	6.1
^{106}Pd /^{107}Ag	382.7	−127.7	39.3	92.1	− 6.5	10.5
^{108}Cd /^{107}Ag	576.1	−249.9	39.3	142.1	− 30.6	6.2
^{108}Pd /^{109}Ag	407.6	−59.1	41.6	100.1	− 37.2	12.4
^{110}Cd /^{109}Ag	606.5	−283.4	41.6	109.2	− 32.2	11.7
^{110}Pd /^{111}Ag	334.3	−22.4	40.7	92.1	− 32.0	12.5
^{112}Cd /^{111}Ag	543.9	−265.6	40.7	82.7	− 21.1	12.4

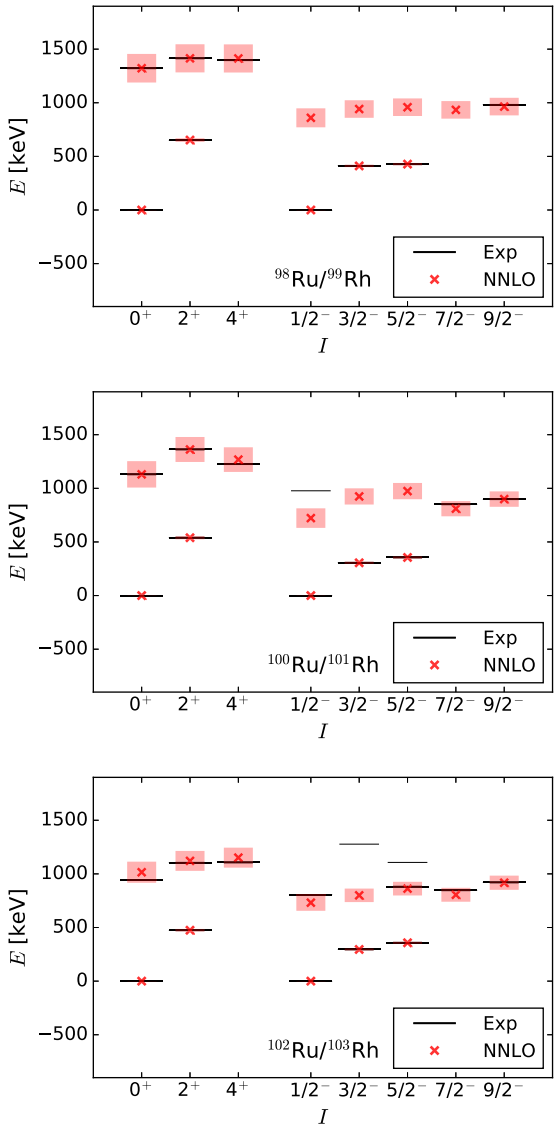

FIG. 3. NNLO energy spectra of Ru/Rh systems. Rh is described as a proton in a $j^\pi = \frac{1}{2}^-$ orbital coupled to a Ru core. Thick black lines denote states employed to fit the LECs while thin black lines denote states with a definitely known spin or a single tentative spin-parity assignment. Red crosses and shaded areas denote theoretical predictions and uncertainties, respectively.

From the power counting, the next-to-next-to-next-to-leading order (N3LO) corrections to the energies are expected to scale as ε^3, see Eq. (31). The uncertainties associated with the NNLO energies are quantified by using this estimate and the Bayesian method described in the previous section as

$$\Delta E_{\mathrm{NNLO}}(I^\pi) = \omega_1 \delta(I^\pi), \tag{43}$$

where δ comes from intervals with a 68% DOB. Results within the EFT are in good agreement with experimental data and can help with spin-parity assignments. For example, two states at about 1 MeV in ^{101}Rh both have tentative spin-parity assignments of $\frac{3}{2}^-$ and $\frac{5}{2}^-$, in agreement with the EFT. Similarly, four states around 1 MeV in ^{99}Rh have one or two tentative spin assignments from the set $\frac{1}{2}$, $\frac{3}{2}$, $\frac{5}{2}$, and $\frac{7}{2}$. The EFT suggests that these are negative parity states.

The comparison of Figs. 4 and 5 shows that silver isotopes can be described either as a proton particle or a proton hole coupled to palladium or cadmium, respectively. In the latter case, theoretical uncertainties are larger than in the former, possibly because cadmium isotopes have a lower breakdown scale for vibrations [36].

To illustrate the systematic improvement of the EFT we show the LO, NLO, and NNLO energy spectra of the ^{108}Pd /^{109}Ag system in Fig. 6. The accuracy (agreement with data) and the precision (decrease of theoretical uncertainties) increase with increasing order of the EFT. However, this comes at the cost of reduced predictive power as an increasing number of LECs need to be adjusted to data.

III. $E2$ OBSERVABLES

$E2$ transitions and moments result from the minimal and nonminimal coupling of the effective degrees of freedom to gauge fields and electric fields, respectively. Due to Siegert's theorem, coupling to gauge fields can also be rewritten as nonminimal couplings. The $E2$ operator is a spherical tensor of rank two. In this study we are interested in the reduced $E2$ strengths for transitions between states differing by none or one phonon, and the static $E2$ moments. The relevant terms of the $E2$ operator for the calculation of these observables are [36]

$$\hat{Q}_\mu = Q_0(d^\dagger_\mu + \tilde{d}_\mu) + Q_1(d^\dagger \otimes \tilde{d})^{(2)}_\mu. \tag{44}$$

Here, Q_0 and Q_1 are LECs that must be fit to data. From the power counting one expects Q_1 to scale as

$$Q_1 \sim \sqrt{\frac{\omega_1}{\Lambda}}\, Q_0 \sim \sqrt{\frac{1}{3}}\, Q_0. \tag{45}$$

For the odd-mass nuclei we consider, the $j = \frac{1}{2}$ orbital must couple to boson degrees of freedom to obtain a rank-two tensor. Thus, we could replace $Q_{0,1}$ in Eq. (44) by the linear combination $q_{0,1} + \tilde{q}_{0,1}\hat{n}$ to include fermion effects. Based on the power counting [recall the discussion of the Hamiltonians (15) and (17)], the terms proportional to $\hat{n}$ are subleading corrections. This agrees with our expectations: $B(E2)$ strengths associated with collective quadrupole transitions in even-even nuclei are about tens of Weisskopf units in size and therefore much larger than single-particle effects. Here, we limit ourselves to the leading terms that change and preserve phonon numbers. In Eq. (44) the corresponding operators are proportional to Q_0 and Q_1, respectively.

The reduced $E2$ strength or $B(E2)$ value for the transition between the initial and final states $|i\rangle$ and $|f\rangle$, respectively, is

$$B(E2; i \to f) = \frac{|\langle f||\hat{Q}||i\rangle|^2}{2I_i + 1}. \tag{46}$$

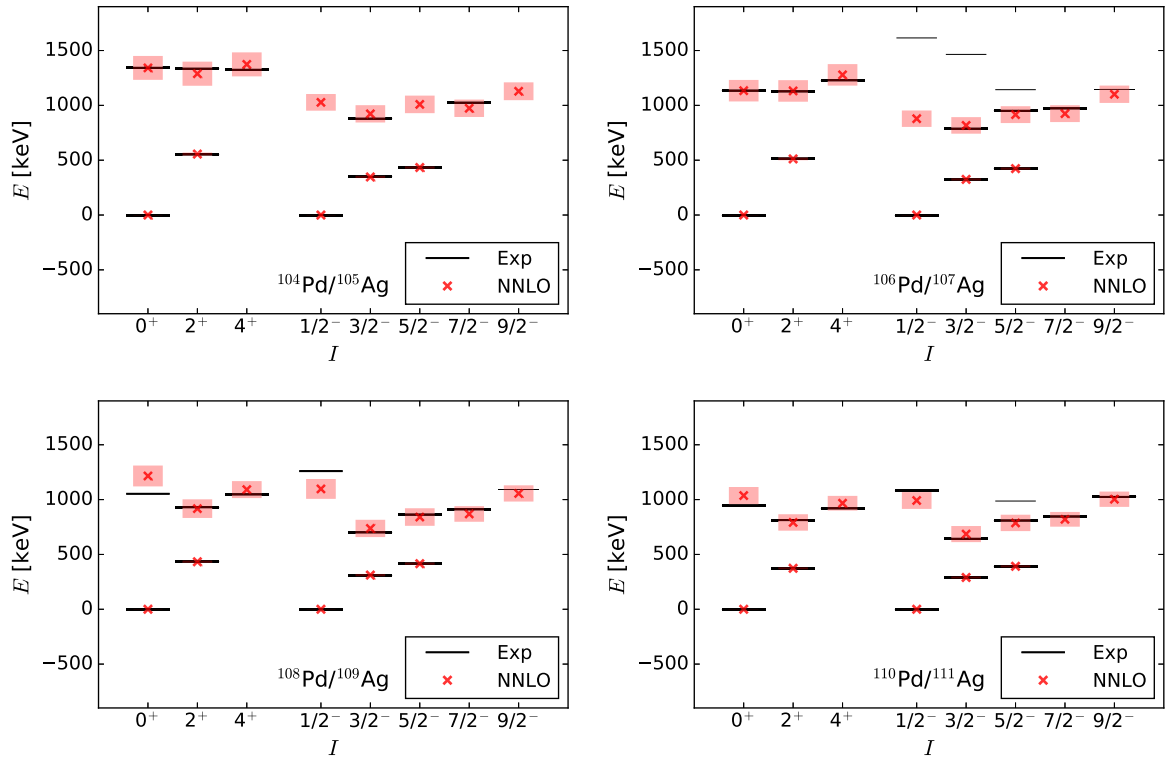

FIG. 4. NNLO energy spectra of Pd/Ag systems. Ag is described as a proton in a $j^\pi = \frac{1}{2}^-$ orbital coupled to a Pd core. Thick black lines denote states employed to fit the LECs while thin black lines denote states with a definitely known spin or a single tentative spin-parity assignment. Red crosses and shaded areas denote theoretical predictions and uncertainties, respectively.

Here,

$$\langle f||\hat{O}||i\rangle = \frac{\sqrt{2I_f+1}}{C^{I_f M_f}_{I_i M_i \lambda M_f - M_i}} \langle f|\hat{O}_{M_f-M_i}|i\rangle \tag{47}$$

is the reduced matrix element of an spherical operator $\hat{O}$ of rank λ. The static $E2$ moment of the state I_i is defined as [9]

$$Q(I_i) = \sqrt{\frac{16\pi}{5}} \frac{C^{II}_{II20}}{\sqrt{2I+1}} \langle I_i||\hat{Q}||I_i\rangle. \tag{48}$$

This definition is consistent when comparing the diagonal reduced matrix elements of the $E2$ operator in ^{106}Pd and ^{108}Pd reported in Ref. [66] and the static $E2$ moments for the same nuclei reported in Ref. [67].

A. Phonon-annihilating transition strengths

The power counting establishes the transitions between states differing by one phonon as the strongest $E2$ observables. In what follows we discuss transitions in which one phonon is annihilated. The term proportional to Q_0 in the $E2$ operator (44) couples states that differ by one phonon; thus, the $E2$ transition strengths for one-phonon decays are governed by this LEC. The reduced matrix elements required for their calculation are

$$\langle I'; N-1; 0||\hat{Q}||I; N; 0\rangle = Q_0\sqrt{N}\Pi_I \text{ for } N = 1,2,$$
$$\left\langle I'; N-1; \tfrac{1}{2}\middle||\hat{Q}\middle||I; NJ; \tfrac{1}{2}\right\rangle$$
$$= \begin{cases} Q_0\Pi_I & \text{for} \quad N=1 \\ Q_0(-1)^{I'+\frac{1}{2}}\sqrt{2}\Pi_{I'JI}\begin{Bmatrix} 2 & 2 & J \\ \frac{1}{2} & I & I' \end{Bmatrix} & \text{for} \quad N=2. \end{cases} \tag{49}$$

Here we used the shorthand

$$\Pi_{ab\ldots c} \equiv \sqrt{(2a+1)(2b+1)\cdots(2c+1)}. \tag{50}$$

Table II lists the reduced matrix elements for the transitions of interest resulting from Eq. (49) in terms of the LEC Q_0. NLO corrections to these matrix elements are expected to scale as ε. As a cautionary note we remark that identical units have to be employed when fitting Q_0 to experimental data, and recall that Weisskopf units depend on the number of nucleons A for $E2$ transitions.

Tables III–VI show LO results for phonon-annihilating $E2$ transition strengths in the ^{102}Ru /^{103}Rh, ^{106}Pd /^{107}Ag, ^{108}Pd /^{109}Ag, and ^{110}Cd /^{109}Ag, respectively. The uncertainties in these tables are quantified as $Q_0^2\delta$, and δ comes from 68% DOB intervals. For the other systems studied in this work, data on $E2$ transition strengths are insufficient to conduct a similar analysis. It would be valuable to measure $E2$ transition strengths in those systems in order to further test the EFT. Most of the available data on $E2$ transition strengths were employed to fit the single LEC Q_0. The

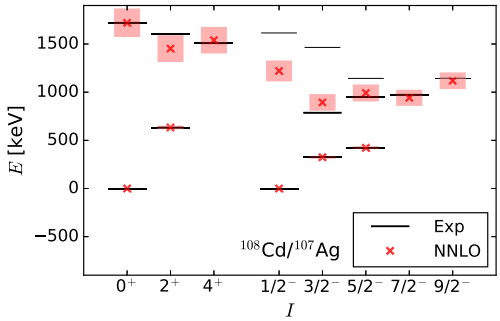

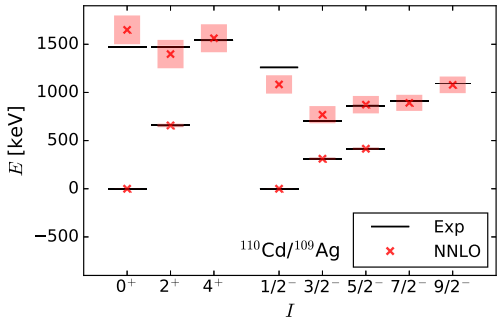

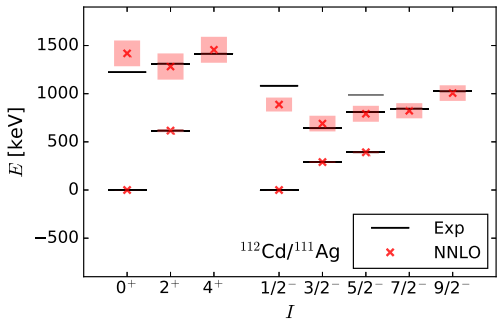

FIG. 5. NNLO energy spectra of Cd/Ag systems. Ag is described as a proton hole in a $j^\pi = \frac{1}{2}^-$ orbital coupled to a Cd core. Thick black lines denote states employed to fit the LECs while thin black lines denote states with a definitely known spin or a single tentative spin-parity assignment. Red crosses and shaded areas denote theoretical predictions and uncertainties, respectively.

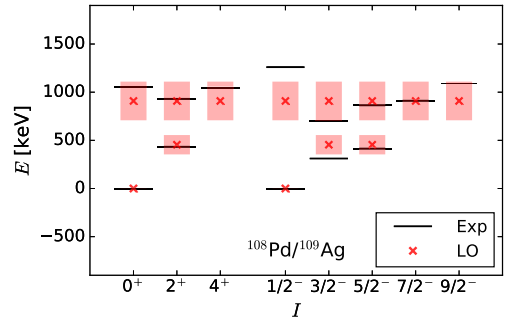

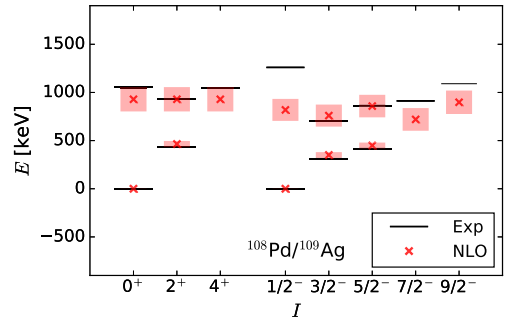

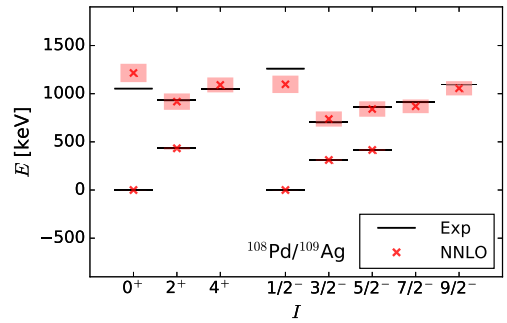

FIG. 6. LO (top), NLO (center), and NNLO (bottom) energy spectra of the ^{108}Pd/^{109}Ag system. The systematic improvement inherent to EFT approaches is evident.

only exception was the $(\frac{1}{2})_2^- \to (\frac{5}{2})_1^-$ transition strength in ^{103}Rh, which was excluded due to its unexpectedly large value. The values of Q_0 for the ^{102}Ru/^{103}Rh, ^{106}Pd/^{107}Ag, ^{108}Pd/^{109}Ag, and ^{110}Cd/^{109}Ag systems are 0.28, 0.32, 0.32, and 0.27 eb, respectively. Note that the transition strengths in ^{109}Ag can be described employing either ^{108}Pd or ^{110}Cd as a core. Both descriptions agree with each other within theoretical uncertainties.

B. Static moments and phonon-conserving transition strengths

The term proportional to Q_1 in the $E2$ operator (44) couples states with the same number of phonons. Thus, Q_1 enters in the LO calculation of static $E2$ moments. The reduced matrix elements associated with these observables are

$$\langle I';N;0||\hat{Q}||I;N;0\rangle = \begin{cases} 0 & \text{for} \quad N=0 \\ Q_1\Pi_I & \text{for} \quad N=1 \\ 2Q_1\sqrt{5}\Pi_{I'I}\begin{Bmatrix} 2 & 2 & 2 \\ 2 & I & I' \end{Bmatrix} & \text{for} \quad N=2, \end{cases}$$

$$\langle I';NJ';\tfrac{1}{2}||\hat{Q}||I;NJ;\tfrac{1}{2}\rangle = \begin{cases} 0 & \text{for} \quad N=0 \\ Q_1(-1)^{I+\frac{1}{2}}\sqrt{5}\Pi_{I'I}\begin{Bmatrix} 2 & 2 & 2 \\ \frac{1}{2} & I & I' \end{Bmatrix} & \text{for} \quad N=1 \\ 2Q_1(-1)^{I+\frac{1}{2}}\sqrt{5}\Pi_{I'J'IJ}\begin{Bmatrix} 2 & 2 & 2 \\ 2 & J' & J \end{Bmatrix}\begin{Bmatrix} 2 & J' & J \\ \frac{1}{2} & I & I' \end{Bmatrix} & \text{for} \quad N=2. \end{cases} \tag{51}$$

TABLE II. Reduced matrix elements relevant for phonon-annihilating transitions in units of Q_0.

System	$I_i \to I_f$	$\langle f \Vert \hat{Q} \Vert i \rangle$
Even-even	$2_1 \to 0_1$	$\sqrt{5}$
Even-even	$0_2 \to 2_1$	$\sqrt{2}$
Even-even	$2_2 \to 2_1$	$\sqrt{10}$
Even-even	$4_1 \to 2_1$	$\sqrt{18}$
Odd-mass	$\frac{3}{2}_1 \to \frac{1}{2}_1$	2
Odd-mass	$\frac{5}{2}_1 \to \frac{1}{2}_1$	$\sqrt{6}$
Odd-mass	$\frac{1}{2}_2 \to \frac{3}{2}_1$	$-\sqrt{\frac{8}{5}}$
Odd-mass	$\frac{1}{2}_2 \to \frac{5}{2}_1$	$\sqrt{\frac{12}{5}}$
Odd-mass	$\frac{3}{2}_2 \to \frac{3}{2}_1$	$\sqrt{\frac{28}{5}}$
Odd-mass	$\frac{3}{2}_2 \to \frac{5}{2}_1$	$\sqrt{\frac{12}{5}}$
Odd-mass	$\frac{5}{2}_2 \to \frac{3}{2}_1$	$-\sqrt{\frac{12}{5}}$
Odd-mass	$\frac{5}{2}_2 \to \frac{5}{2}_1$	$\sqrt{\frac{48}{5}}$
Odd-mass	$\frac{7}{2}_1 \to \frac{3}{2}_1$	$\sqrt{\frac{72}{5}}$
Odd-mass	$\frac{7}{2}_1 \to \frac{5}{2}_1$	$\sqrt{\frac{8}{5}}$
Odd-mass	$\frac{9}{2}_1 \to \frac{5}{2}_1$	$\sqrt{20}$

TABLE III. Reduced transition probabilities for phonon-annihilating $E2$ transitions in the ^{102}Ru / ^{103}Rh system in Weisskopf units. The uncertainty was quantified from 68% DOB intervals.

Nucleus	$I_i^\pi \to I_f^\pi$	$B(E2)_{\text{expt}}$	$B(E2)_{\text{EFT}}$
^{102}Ru	$2_1^+ \to 0_1^+$	45(1)	27(9)
^{102}Ru	$0_2^+ \to 2_1^+$	35(6)	55(18)
^{102}Ru	$2_2^+ \to 2_1^+$	32(5)	55(18)
^{102}Ru	$4_1^+ \to 2_1^+$	66(11)	55(18)
^{103}Rh	$\frac{3}{2}_1^- \to \frac{1}{2}_1^-$	36(4)	27(9)
^{103}Rh	$\frac{5}{2}_1^- \to \frac{1}{2}_1^-$	44(3)	27(9)
^{103}Rh	$\frac{1}{2}_2^- \to \frac{3}{2}_1^-$		22(18)
^{103}Rh	$\frac{1}{2}_2^- \to \frac{5}{2}_1^-$	486(90)	32(18)
^{103}Rh	$\frac{3}{2}_2^- \to \frac{3}{2}_1^-$		38(18)
^{103}Rh	$\frac{3}{2}_2^- \to \frac{5}{2}_1^-$		16(18)
^{103}Rh	$\frac{5}{2}_2^- \to \frac{3}{2}_1^-$	3(1)	11(18)
^{103}Rh	$\frac{5}{2}_2^- \to \frac{5}{2}_1^-$	4(1)	43(18)
^{103}Rh	$\frac{7}{2}_1^- \to \frac{3}{2}_1^-$	34(11)	48(18)
^{103}Rh	$\frac{7}{2}_1^- \to \frac{5}{2}_1^-$		5(18)
^{103}Rh	$\frac{9}{2}_1^- \to \frac{5}{2}_1^-$	46(7)	54(18)

TABLE IV. Reduced transition probabilities for phonon-annihilating $E2$ transitions in the ^{106}Pd / ^{107}Ag system in Weisskopf units. The uncertainty was quantified from 68% DOB intervals.

Nucleus	$I_i^\pi \to I_f^\pi$	$B(E2)_{\text{expt}}$	$B(E2)_{\text{EFT}}$
^{106}Pd	$2_1^+ \to 0_1^+$	44(1)	35(12)
^{106}Pd	$0_2^+ \to 2_1^+$	35(8)	69(23)
^{106}Pd	$2_2^+ \to 2_1^+$	44(4)	69(23)
^{106}Pd	$4_1^+ \to 2_1^+$	76(11)	69(23)
^{107}Ag	$\frac{3}{2}_1^- \to \frac{1}{2}_1^-$	42(4)	34(11)
^{107}Ag	$\frac{5}{2}_1^- \to \frac{1}{2}_1^-$	43(3)	34(11)
^{107}Ag	$\frac{1}{2}_2^- \to \frac{3}{2}_1^-$		27(23)
^{107}Ag	$\frac{1}{2}_2^- \to \frac{5}{2}_1^-$		41(23)
^{107}Ag	$\frac{3}{2}_2^- \to \frac{3}{2}_1^-$		48(23)
^{107}Ag	$\frac{3}{2}_2^- \to \frac{5}{2}_1^-$		20(23)
^{107}Ag	$\frac{5}{2}_2^- \to \frac{3}{2}_1^-$		14(23)
^{107}Ag	$\frac{5}{2}_2^- \to \frac{5}{2}_1^-$		55(23)
^{107}Ag	$\frac{7}{2}_1^- \to \frac{3}{2}_1^-$		62(23)
^{107}Ag	$\frac{7}{2}_1^- \to \frac{5}{2}_1^-$		7(23)
^{107}Ag	$\frac{9}{2}_1^- \to \frac{5}{2}_1^-$		68(23)

The static $E2$ moments and reduced matrix elements required to calculate the $E2$ strengths for transitions between two-phonon states at LO are given in units of Q_1 in Tables VII and VIII, respectively. NLO corrections to these quantities are expected to scale as ε.

Our results for static $E2$ moments in the ^{102}Ru / ^{103}Rh, ^{106}Pd / ^{107}Ag, and ^{108}Pd / ^{109}Ag systems are listed in

TABLE V. Reduced transition probabilities for phonon-annihilating $E2$ transitions in the ^{108}Pd / ^{109}Ag system in Weisskopf units. The uncertainty was quantified from 68% DOB intervals.

Nucleus	$I_i^\pi \to I_f^\pi$	$B(E2)_{\text{expt}}$	$B(E2)_{\text{EFT}}$
^{108}Pd	$2_1^+ \to 0_1^+$	49(1)	34(11)
^{108}Pd	$0_2^+ \to 2_1^+$	52(5)	69(23)
^{108}Pd	$2_2^+ \to 2_1^+$	71(5)	69(23)
^{108}Pd	$4_1^+ \to 2_1^+$	73(8)	69(23)
^{109}Ag	$\frac{3}{2}_1^- \to \frac{1}{2}_1^-$	40(40)	34(11)
^{109}Ag	$\frac{5}{2}_1^- \to \frac{1}{2}_1^-$	41(6)	34(11)
^{109}Ag	$\frac{1}{2}_2^- \to \frac{3}{2}_1^-$		27(23)
^{109}Ag	$\frac{1}{2}_2^- \to \frac{5}{2}_1^-$		41(23)
^{109}Ag	$\frac{3}{2}_2^- \to \frac{3}{2}_1^-$	49(24)	47(23)
^{109}Ag	$\frac{3}{2}_2^- \to \frac{5}{2}_1^-$		20(23)
^{109}Ag	$\frac{5}{2}_2^- \to \frac{3}{2}_1^-$	8(4)	14(23)
^{109}Ag	$\frac{5}{2}_2^- \to \frac{5}{2}_1^-$	10(7)	54(23)
^{109}Ag	$\frac{7}{2}_1^- \to \frac{3}{2}_1^-$		61(23)
^{109}Ag	$\frac{7}{2}_1^- \to \frac{5}{2}_1^-$		7(23)
^{109}Ag	$\frac{9}{2}_1^- \to \frac{5}{2}_1^-$		68(23)

TABLE VI. Reduced transition probabilities for phonon-annihilating $E2$ transitions in the ^{110}Cd/^{109}Ag system in Weisskopf units. The uncertainty was quantified from 68% DOB intervals.

Nucleus	$I_i^\pi \to I_f^\pi$	$B(E2)_{\text{expt}}$	$B(E2)_{\text{EFT}}$
^{110}Cd	$2_1^+ \to 0_1^+$	27(1)	23(8)
^{110}Cd	$0_2^+ \to 2_1^+$		46(15)
^{110}Cd	$2_2^+ \to 2_1^+$	30(5)	46(15)
^{110}Cd	$4_1^+ \to 2_1^+$	42(9)	46(15)
^{109}Ag	$\frac{3}{2}{}_1^- \to \frac{1}{2}{}_1^-$	40(40)	23(8)
^{109}Ag	$\frac{5}{2}{}_1^- \to \frac{1}{2}{}_1^-$	41(6)	23(8)
^{109}Ag	$\frac{1}{2}{}_2^- \to \frac{3}{2}{}_1^-$		19(16)
^{109}Ag	$\frac{1}{2}{}_2^- \to \frac{5}{2}{}_1^-$		28(16)
^{109}Ag	$\frac{3}{2}{}_2^- \to \frac{3}{2}{}_1^-$	49(24)	33(16)
^{109}Ag	$\frac{3}{2}{}_2^- \to \frac{5}{2}{}_1^-$		14(16)
^{109}Ag	$\frac{5}{2}{}_2^- \to \frac{3}{2}{}_1^-$	8(4)	9(16)
^{109}Ag	$\frac{5}{2}{}_2^- \to \frac{5}{2}{}_1^-$	10(7)	37(16)
^{109}Ag	$\frac{7}{2}{}_1^- \to \frac{3}{2}{}_1^-$		42(16)
^{109}Ag	$\frac{7}{2}{}_1^- \to \frac{5}{2}{}_1^-$		5(16)
^{109}Ag	$\frac{9}{2}{}_1^- \to \frac{5}{2}{}_1^-$		47(16)

Table IX, where the theoretical uncertainty for the state I^π was quantified as $\sqrt{16\pi/5(2I+1)}C^{II}_{II20}Q_0\delta$ [in agreement with the definition given in Eq. (48)], with δ from 68% DOB intervals. All available data from Refs. [66,67] were used to fit the LEC Q_1 through weighted averages. Note that, for the studied systems, the values for $|Q_1/Q_0|$ of 0.87, 0.92, and 1.04, although large, are consistent with the expected value of

TABLE VII. Static $E2$ moments of states up to the two-phonon level in units of Q_1. The index i denotes the position of the excited state.

System	I_i	$Q(I_i)$
Even-even	2_1	$8\sqrt{\frac{2\pi}{35}}$
Even-even	2_2	$-\frac{24}{7}\sqrt{\frac{2\pi}{35}}$
Even-even	4_1	$16\sqrt{\frac{2\pi}{35}}$
Odd-mass	$\frac{3}{2}{}_1$	$\frac{28}{5}\sqrt{\frac{2\pi}{35}}$
Odd-mass	$\frac{5}{2}{}_1$	$8\sqrt{\frac{2\pi}{35}}$
Odd-mass	$\frac{3}{2}{}_2$	$-\frac{12}{5}\sqrt{\frac{2\pi}{35}}$
Odd-mass	$\frac{5}{2}{}_2$	$-\frac{24}{7}\sqrt{\frac{2\pi}{35}}$
Odd-mass	$\frac{7}{2}{}_1$	$\frac{44}{3}\sqrt{\frac{2\pi}{35}}$
Odd-mass	$\frac{9}{2}{}_1$	$16\sqrt{\frac{2\pi}{35}}$

TABLE VIII. Reduced matrix elements relevant for phonon-conserving $E2$ transitions in units of Q_1.

System	$I_i \to I_f$	$\langle f\|\|\hat{Q}\|\|i\rangle$
Even-even	$2_2 \to 0_2$	4
Even-even	$4_1 \to 2_2$	$\frac{24}{7}$
Odd-mass	$\frac{5}{2}{}_1 \to \frac{3}{2}{}_1$	$-\sqrt{\frac{24}{5}}$
Odd-mass	$\frac{3}{2}{}_2 \to \frac{1}{2}{}_2$	$\sqrt{\frac{64}{5}}$
Odd-mass	$\frac{5}{2}{}_2 \to \frac{1}{2}{}_2$	$\sqrt{\frac{96}{5}}$
Odd-mass	$\frac{5}{2}{}_2 \to \frac{3}{2}{}_2$	$\sqrt{\frac{216}{245}}$
Odd-mass	$\frac{7}{2}{}_1 \to \frac{3}{2}{}_2$	$\sqrt{\frac{2304}{245}}$
Odd-mass	$\frac{7}{2}{}_1 \to \frac{5}{2}{}_2$	$\sqrt{\frac{256}{245}}$
Odd-mass	$\frac{9}{2}{}_1 \to \frac{5}{2}{}_2$	$\sqrt{\frac{640}{49}}$
Odd-mass	$\frac{9}{2}{}_1 \to \frac{7}{2}{}_1$	$-\sqrt{\frac{880}{147}}$

0.58 for this quantity. For comparison, a description of ^{109}Ag as a proton-hole coupled to a ^{110}Cd core was also performed. This description is consistent with the one describing ^{109}Ag

TABLE IX. Static $E2$ moments in some systems in eb. The uncertainty was quantified from 68% DOB intervals.

Nucleus	I_i^π	Q_{expt}	Q_{EFT}
^{102}Ru	2_1^+	$-0.63(3)$	$-0.41(6)$
^{102}Ru	2_2^+		0.18(18)
^{102}Ru	4_1^+		$-0.82(14)$
^{103}Rh	$\frac{3}{2}{}_1^-$	$-0.3(2)$	$-0.29(7)$
^{103}Rh	$\frac{5}{2}{}_1^-$	$-0.4(2)$	$-0.41(6)$
^{106}Pd	2_1^+	$-0.54(4)$	$-0.50(7)$
^{106}Pd	2_2^+	0.39(6)	0.21(20)
^{106}Pd	4_1^+	$-0.79(11)$	$-1.00(17)$
^{107}Ag	$\frac{3}{2}{}_1^-$		$-0.35(8)$
^{107}Ag	$\frac{5}{2}{}_1^-$		$-0.50(7)$
^{108}Pd	2_1^+	$-0.56(3)$	$-0.57(7)$
^{108}Pd	2_2^+	0.73(9)	0.24(20)
^{108}Pd	4_1^+	$-0.78(11)$	$-1.14(17)$
^{109}Ag	$\frac{3}{2}{}_1^-$	$-0.7(3)$	$-0.40(8)$
^{109}Ag	$\frac{5}{2}{}_1^-$	$-0.3(3)$	$-0.57(6)$
^{110}Cd	2_1^+	$-0.39(3)$	$-0.57(7)$
^{110}Cd	2_2^+		0.24(17)
^{110}Cd	4_1^+		-1.12(14)
^{109}Ag	$\frac{3}{2}{}_1^-$	$-0.7(3)$	$-0.39(6)$
^{109}Ag	$\frac{5}{2}{}_1^-$	$-0.3(3)$	$-0.56(6)$

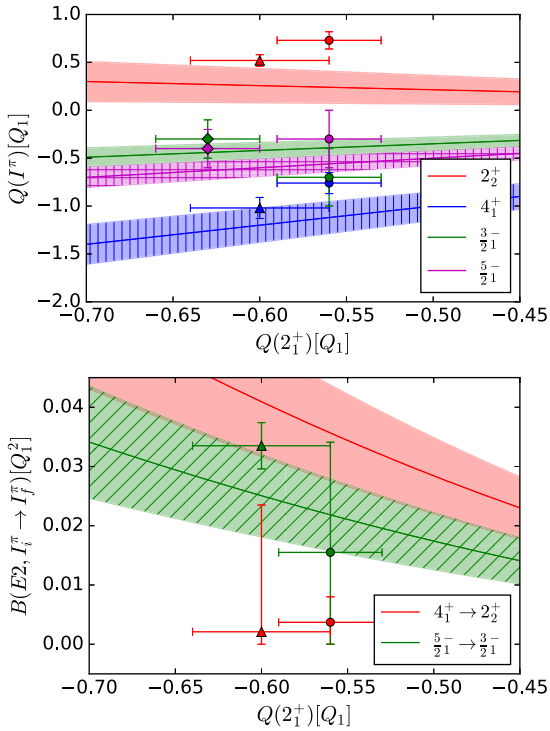

FIG. 7. Static $E2$ moments (top) and $E2$ transitions strengths (bottom) as functions of $Q(2_1^+)$. The uncertainty quantified from 68% DOB intervals is shown as error bands. Data for the ^{102}Ru /^{103}Rh, ^{106}Pd /^{107}Ag, and ^{108}Pd /^{109}Ag systems are shown as diamonds, triangles, and circles, respectively.

as a proton coupled to a ^{108}Pd core. In the former case $|Q_1/Q_0| = 1.23$, probably larger than naively expected from the EFT.

The expressions in Tables VII and VIII can be used to relate different $E2$ observables. As examples, static $E2$ moments and $E2$ transition strengths are plotted as functions of $Q(2_1^+)$ in Fig. 7. The theoretical uncertainties associated with these quantities, quantified via 68% DOB intervals, are represented by bands. In the top part of the figure, the static $E2$ moments of the 2_2^+, 4_1^+, $(\frac{3}{2})_1^-$, and $(\frac{5}{2})_1^-$ states are shown as red, blue, green, and purple lines, respectively. In the bottom of the figure, the $E2$ transition strengths for the $4_1^+ \to 2_2^+$ and $(\frac{5}{2})_1^- \to (\frac{3}{2})_1^-$ transitions are shown as red and green lines, respectively. Experimental data for the ^{102}Ru /^{103}Rh, ^{106}Pd /^{107}Ag, and ^{108}Pd /^{109}Ag systems are shown in the figure as colored diamonds, triangles, and circles, respectively. For these systems, the relations plotted in Fig. 7 are fulfilled except for those involving the 2_2^+ state.

IV. $M1$ OBSERVABLES

The magnetic dipole ($M1$) operator is a spherical tensor of rank one. In our EFT, the simplest rank-one operator is

$$\hat{\mu}_\mu = \mu_d \hat{\mathbf{J}}_\mu + \mu_a \hat{\mathbf{j}}_\mu + [(d^\dagger + \tilde{d}) \otimes (\mu_{d1} \hat{\mathbf{J}} + \mu_{a1} \hat{\mathbf{j}})]^{(1)}_\mu. \quad (52)$$

The first and second terms on the right-hand side of Eq. (52) preserve the phonon number, and enter in the LO calculation of static $M1$ moments and phonon-conserving $M1$ transition strengths. The last two terms enter in the LO calculation of phonon-changing $M1$ transition strengths.

Experimental data show that the typical size for the static $M1$ moment of the even-even 2_1^+ state is about one nuclear magneton μ_N. This observation and the fact that, in even-even nuclei,

$$\langle I||\hat{\mathbf{J}}||I\rangle = \sqrt{I(I+1)(2I+1)}, \quad (53)$$

allows us to estimate the scale for the LEC μ_d as

$$\mu_d \sim \tfrac{1}{5}\mu_N. \quad (54)$$

The Schmidt value for the magnetic moment of a proton in a $j^\pi = \frac{1}{2}^-$ orbital is $\mu_p \approx -0.26\mu_N$. In contrast to $E2$ phenomena, magnetic properties in vibrational nuclei are not collective, and the contributions of the odd fermion cannot be neglected. As will be shown in what follows, the static $M1$ moment of the $I = \frac{1}{2}$ ground state of the odd-mass nuclei calculated from the operator (52) is $\mu(\frac{1}{2}) = \sqrt{\pi/3}\mu_a$. Thus, we naively estimate the value of μ_a as

$$\mu_a \sim \mu_p. \quad (55)$$

Static $M1$ moments for the ground state in ^{103}Rh, ^{107}Ag, and ^{109}Ag are consistent with this estimate. It is important to realize that the LEC μ_a is neither equal nor simply related to the Schmidt value. In the EFT considered in this work, we couple a fermion with $j^\pi = \frac{1}{2}^-$ (and not a free proton in a p wave) to a collective state. We have no information about any radial wave function of the coupled fermion, and we have no operators to act on its spin and its orbital angular momentum separately. The coupling between the fermion and the core is strong (as the separation energy S considerably exceeds the energy scale ω of core excitations). The result of the coupling is again a collective state, and renormalizations replace "bare" quantities such as the proton's magnetic moment by effective couplings. It is useful to contrast the EFT for vibrations in odd-mass nuclei with halo EFT [28–30,68] for odd-mass nuclei. In halo EFT, a nucleon is very weakly bound to a core, and $S \ll \omega$ holds. The nucleon's Schmidt value is the leading contribution to the total magnetic moment, and subleading corrections are of size $S/\omega \ll 1$ [69,70].

Let us now turn to the phonon-changing terms in Eq. (52) and discuss the size of the LECs μ_{d1} and μ_{a1}. Due to the absence of strong collective effects in $M1$ observables, the naive expectation is that transition matrix elements again are of single-particle size, i.e., similar to μ_N or μ_p. Higher-order corrections to the leading phonon-changing and phonon-preserving terms of the $M1$ operator (52) enter with increasing powers of boson or fermion creation and annihilation operators. We expect them to scale as ε and neglect them in what follows.

The $M1$ reduced transition probabilities and static $M1$ moments are given by [9]

$$B(M1; i \to f) = \frac{|\langle f||\hat{\mu}||i\rangle|^2}{2I_i + 1}, \quad (56)$$

and

$$\mu(I) = \sqrt{\frac{4\pi}{3}} \frac{C^{II}_{II10}}{\sqrt{2I+1}} \langle I||\hat{\mu}||I\rangle, \quad (57)$$

respectively.

A. Static moments and phonon-conserving transition strengths

The LO static $M1$ moments of even-even and odd-mass nuclei can be calculated from the reduced matrix elements of the first and second terms of the $M1$ operator (52). These are

$$\langle I';N;0||\hat{\mu}||I;N;0\rangle = \begin{cases} 0 & \text{for} \quad N=0 \\ \mu_d\sqrt{I(I+1)}\Pi_I & \text{for} \quad N=1 \\ -2\mu_d\sqrt{30}\Pi_{I'I}\begin{Bmatrix}1 & 2 & 2\\ 2 & I & I'\end{Bmatrix} & \text{for} \quad N=2, \end{cases} \tag{58}$$

and

$$\begin{aligned}\left\langle I';N,J';\tfrac{1}{2}\middle|\middle|\hat{\mu}\middle|\middle|I;NJ;\tfrac{1}{2}\right\rangle = &\begin{cases} 0 & \text{for} \quad N=0 \\ -\mu_d(-1)^{I+\frac{1}{2}}\sqrt{30}\Pi_{I'I}\begin{Bmatrix}1 & 2 & 2\\ \frac{1}{2} & I & I'\end{Bmatrix} & \text{for} \quad N=1 \\ 2\mu_d(-1)^{I+\frac{1}{2}}\sqrt{30}\Pi_{I'J'IJ}\begin{Bmatrix}1 & 2 & 2\\ 2 & J' & J\end{Bmatrix}\begin{Bmatrix}1 & J' & J\\ \frac{1}{2} & I & I'\end{Bmatrix} & \text{for} \quad N=2 \end{cases} \\ &+\begin{cases} \mu_a\sqrt{\frac{3}{2}} & \text{for} \quad N=0 \\ -\mu_a(-1)^{I'+\frac{1}{2}}\sqrt{\frac{3}{2}}\Pi_{I'I}\begin{Bmatrix}1 & \frac{1}{2} & \frac{1}{2}\\ 2 & I & I'\end{Bmatrix} & \text{for} \quad N=1 \\ -\mu_a(-1)^{I'+\frac{1}{2}}\sqrt{\frac{3}{2}}\Pi_{I'I}\begin{Bmatrix}1 & \frac{1}{2} & \frac{1}{2}\\ J & I & I'\end{Bmatrix}\delta^J_{J'} & \text{for} \quad N=2. \end{cases}\end{aligned} \tag{59}$$

Results are listed in Table X. These terms of the $M1$ operator (52) couple states with the same number of phonons, and enter in the LO calculation of the allowed phonon-conserving $M1$ transition strengths in odd-mass nuclei. The reduced matrix elements employed to calculate these observables are listed in Table XI.

Our results for static $M1$ moments in the ^{102}Ru$/^{103}$Rh, ^{106}Pd$/^{107}$Ag, and ^{108}Pd$/^{109}$Ag systems, with uncertainties quantified as $\sqrt{4\pi/3(2I+1)}C^{II}_{II10}\mu_d\delta$ [in agreement with the definition given in Eq. (57)], where δ comes from intervals with a 68% DOB, are listed in Table XII. Most experimental values in the table are weighted averages of data from Refs. [66,67,71]. The static $M1$ moment of the $I^\pi = \frac{1}{2}^-$ ground state in ^{103}Rh was taken from Ref. [72]. For each system, we adjusted the LECs μ_d and μ_a to the static $M1$ moments of the even-even 2^+_1 and odd-mass $(\frac{1}{2})^\pi_1$ states, respectively. Notice that the values for μ_d of $0.21\mu_N$, $0.19\mu_N$, and $0.17\mu_N$ in the ^{102}Ru$/^{103}$Rh, ^{106}Pd$/^{107}$Ag, and ^{108}Pd$/^{109}$Ag systems, respectively, are all consistent with the naive estimate $0.2\mu_N$. Similarly, the values for μ_a of $-0.09\mu_N$, $-0.11\mu_N$ and $-0.13\mu_N$ are all consistent with the Schmidt value $\mu_p = -0.26\mu_N$.

Table XIII lists our results for phonon-conserving $M1$ transition strengths in the studied odd-mass nuclei, with uncertainties quantified as $\mu_d^2\delta/(2I_i+1)$, where δ comes from intervals with a 68% DOB. The sparse available data on phonon-conserving $M1$ transition strengths are consistent with the EFT predictions.

B. Phonon-annihilating transition strengths

The last two terms of the $M1$ operator (52) couple states whose number of phonons differ by one. Their reduced matrix elements allow us to calculate phonon-annihilating $M1$ transition strengths at LO. In even-even nuclei, these transitions are higher-order effects, as discussed in Ref. [36]. The reduced matrix elements of these terms in odd-mass nuclei are

$$\begin{aligned}\left\langle I';N-1,J';\tfrac{1}{2}\middle|\middle|\hat{\mu}\middle|\middle|I;NJ;\tfrac{1}{2}\right\rangle = &\begin{cases} 0 & \text{for} \quad N=1 \\ 6\mu_{d1}(-1)^{I+\frac{1}{2}}\sqrt{5}\Pi_{I'IJ}\begin{Bmatrix}2 & 2 & J\\ 2 & 1 & 1\end{Bmatrix}\begin{Bmatrix}I & I' & 1\\ 2 & J & \frac{1}{2}\end{Bmatrix} & \text{for} \quad N=2 \end{cases} \\ &+\begin{cases} -\mu_{a1}(-1)^{I+j}\sqrt{\frac{9}{2}}\Pi_I\begin{Bmatrix}1 & 1 & 2\\ \frac{1}{2} & I & I'\end{Bmatrix} & \text{for} \quad N=1 \\ 3\mu_a\Pi_{I'IJ}\begin{Bmatrix}I' & 2 & \frac{1}{2}\\ I & J & \frac{1}{2}\\ 1 & 2 & 1\end{Bmatrix} & \text{for} \quad N=2. \end{cases}\end{aligned} \tag{60}$$

TABLE X. Static $M1$ moments of states up to the two-phonon level in terms of μ_d and μ_a.

System	I	$\mu(I)$
Even-even	2	$4\sqrt{\frac{\pi}{3}}\mu_d$
Even-even	4	$8\sqrt{\frac{\pi}{3}}\mu_d$
Odd-mass	$\frac{1}{2}$	$\sqrt{\frac{\pi}{3}}\mu_a$
Odd-mass	$\frac{3}{2}$	$\frac{18}{5}\sqrt{\frac{\pi}{3}}\mu_d - \frac{3}{5}\sqrt{\frac{\pi}{3}}\mu_a$
Odd-mass	$\frac{5}{2}$	$4\sqrt{\frac{\pi}{3}}\mu_d + \sqrt{\frac{\pi}{3}}\mu_a$
Odd-mass	$\frac{7}{2}$	$\frac{70}{9}\sqrt{\frac{\pi}{3}}\mu_d - \frac{7}{9}\sqrt{\frac{\pi}{3}}\mu_a$
Odd-mass	$\frac{9}{2}$	$8\sqrt{\frac{\pi}{3}}\mu_d + \sqrt{\frac{\pi}{3}}\mu_a$

The relevant matrix elements for the calculation of these observables in odd-mass nuclei are listed in Table XIV.

In Table XV we present our results for phonon-annihilating $M1$ transition strengths in ^{103}Rh and ^{109}Ag, with uncertainties quantified as $\mu_{a1}^2\delta/(2I_i+1)$, where δ comes from 68% DOB intervals. All available data from Refs. [56,63] were employed to fit the LECs. For ^{103}Rh and ^{109}Ag we find values for μ_{d1} of $0.0\mu_N$ and $0.08\mu_N$, and values for μ_{a1} of $0.68\mu_N$ and $0.76\mu_N$, respectively. The small values for μ_{d1}, although smaller than naively expected, reflect the fact that $M1$ transitions in even-even nuclei are higher-order effects. The values for μ_{a1} are consistent with the naive estimates. Our results are in agreement with the sparse experimental data on phonon-annihilating $M1$ transition strengths.

V. DISCUSSION OF ODD-MASS CADMIUM ISOTOPES

The results presented for spectra, $E2$ moments and transitions, and $M1$ moments and transitions suggest that an EFT approach to odd-mass nuclei yields a consistent description of low-energy data. Admittedly, the agreement between theory and data is also due to the relatively large experimental and theoretical uncertainties. More precise data are necessary to really probe the theory and to motivate the computation of higher-order corrections.

Technically, the EFT we considered falls into the category of "particle-vibrator" models. Very recently, Stuchbery *et al.* [49] measured g factors of the odd isotopes ^{111,113}Cd and found that the specific particle-vibrator model of Ref. [73] failed to capture key aspects of the data. A second attempt to describe these cadmium isotopes was then made within the particle-rotor (PR) model described in Ref. [74].

TABLE XI. Reduced matrix elements relevant for phonon-conserving $M1$ transitions in terms of μ_d and μ_a.

System	$I_i \to I_f$	$\langle f\|\|\hat{\mu}\|\|i\rangle$
Odd-mass	$\frac{5}{2} \to \frac{3}{2}$	$-\sqrt{\frac{12}{5}}\mu_d + \sqrt{\frac{12}{5}}\mu_a$
Odd-mass	$\frac{9}{2} \to \frac{7}{2}$	$-\sqrt{\frac{40}{9}}\mu_d + \sqrt{\frac{40}{9}}\mu_a$

TABLE XII. Static $M1$ moments in the ^{102}Ru /^{103}Rh, ^{106}Pd /^{107}Ag, and ^{108}Pd /^{109}Ag systems in units of μ_N. Values marked with an asterisk were employed to fit the LECs. The uncertainty was quantified from 68% DOB intervals.

Nucleus	I_i^π	$\mu_{\rm expt}(I_i^\pi)$	$\mu_{\rm EFT}(I_i^\pi)$
^{102}Ru	2_1^+	0.85(3)*	0.85(5)
^{102}Ru	2_2^+		0.85(10)
^{102}Ru	4_1^+		1.70(8)
^{103}Rh	$\frac{1}{2}{}_1^-$	−0.088*	−0.088
^{103}Rh	$\frac{3}{2}{}_1^-$	0.77(7)	0.81(5)
^{103}Rh	$\frac{5}{2}{}_1^-$	1.08(4)	0.76(5)
^{103}Rh	$\frac{7}{2}{}_1^-$	2.0(6)	1.7(1)
^{103}Rh	$\frac{9}{2}{}_1^-$	2.8(5)	1.6(1)
^{106}Pd	2_1^+	0.79(2)*	0.79(5)
^{106}Pd	2_2^+	0.71(10)	0.79(10)
^{106}Pd	4_1^+	1.8(4)	1.58(8)
^{107}Ag	$\frac{1}{2}{}_1^-$	−0.11*	−0.11
^{107}Ag	$\frac{3}{2}{}_1^-$	0.98(9)	0.78(5)
^{107}Ag	$\frac{5}{2}{}_1^-$	1.02(9)	0.68(4)
^{107}Ag	$\frac{7}{2}{}_1^-$		1.6(1)
^{107}Ag	$\frac{9}{2}{}_1^-$		1.5(1)
^{108}Pd	2_1^+	0.71(2)*	0.71(4)
^{108}Pd	2_2^+		0.71(9)
^{108}Pd	4_1^+		1.42(7)
^{109}Ag	$\frac{1}{2}{}_1^-$	−0.13*	−0.13
^{109}Ag	$\frac{3}{2}{}_1^-$	1.10(10)	0.72(5)
^{109}Ag	$\frac{5}{2}{}_1^-$	0.85(8)	0.58(4)
^{109}Ag	$\frac{7}{2}{}_1^-$		1.5(1)
^{109}Ag	$\frac{9}{2}{}_1^-$		1.3(1)

TABLE XIII. Reduced transition probabilities for phonon-conserving $M1$ transitions in Weisskopf units. The uncertainty was quantified from 68% DOB intervals.

Nucleus	$I_i^\pi \to I_f^\pi$	$B(M1)_{\rm expt}$	$B(M1)_{\rm EFT}$
^{103}Rh	$\frac{5}{2}{}_1^- \to \frac{3}{2}{}_1^-$		0.034(2)
^{103}Rh	$\frac{5}{2}{}_2^- \to \frac{3}{2}{}_2^-$		0.034(5)
^{103}Rh	$\frac{9}{2}{}_1^- \to \frac{7}{2}{}_1^-$		0.038(3)
^{107}Ag	$\frac{5}{2}{}_1^- \to \frac{3}{2}{}_1^-$	0.033(4)	0.036(2)
^{107}Ag	$\frac{5}{2}{}_2^- \to \frac{3}{2}{}_2^-$		0.036(4)
^{107}Ag	$\frac{9}{2}{}_1^- \to \frac{7}{2}{}_1^-$		0.040(2)
^{109}Ag	$\frac{5}{2}{}_1^- \to \frac{3}{2}{}_1^-$	0.043(7)	0.036(2)
^{109}Ag	$\frac{5}{2}{}_2^- \to \frac{3}{2}{}_2^-$		0.036(3)
^{109}Ag	$\frac{9}{2}{}_1^- \to \frac{7}{2}{}_1^-$		0.040(2)

TABLE XIV. Reduced matrix elements relevant for phonon-annihilating $M1$ transitions in terms of μ_{d1} and μ_{a1}.

System	$I_i \to I_f$	$\langle f\|\|\hat{\mu}\|\|i\rangle$
Odd-mass	$\frac{3}{2}_1 \to \frac{1}{2}_1$	$-\sqrt{\frac{3}{2}}\mu_{a1}$
Odd-mass	$\frac{1}{2}_2 \to \frac{3}{2}_1$	$\sqrt{\frac{3}{5}}\mu_{a1}$
Odd-mass	$\frac{3}{2}_2 \to \frac{3}{2}_1$	$-\frac{3}{5}\sqrt{42}\mu_{d1} + \frac{1}{5}\sqrt{42}\mu_{a1}$
Odd-mass	$\frac{3}{2}_2 \to \frac{5}{2}_1$	$-\frac{1}{5}\sqrt{42}\mu_{d1} - \frac{1}{10}\sqrt{42}\mu_{a1}$
Odd-mass	$\frac{5}{2}_2 \to \frac{3}{2}_1$	$\frac{1}{5}\sqrt{42}\mu_{d1} + \frac{1}{10}\sqrt{42}\mu_{a1}$
Odd-mass	$\frac{5}{2}_2 \to \frac{5}{2}_1$	$-\frac{14}{5}\sqrt{3}\mu_{d1} - \frac{2}{5}\sqrt{3}\mu_{a1}$
Odd-mass	$\frac{7}{2}_1 \to \frac{5}{2}_1$	$-\sqrt{\frac{27}{5}}\mu_{a1}$

What would an EFT approach yield for these isotopes? The ^{111,113}Cd nuclei have $I^\pi = \frac{1}{2}^+$ ground states, and some low-lying levels can be viewed as the result of a $j^\pi = \frac{1}{2}^+$ neutron coupled to the collective excitations of ^{110,112}Cd. In addition to the $j^\pi = \frac{1}{2}^+$ orbital, one also has to include a very-low-lying $j^\pi = \frac{5}{2}^+$ orbital in the description. Let the fermion creation operators $a^\dagger_\nu$ with $\nu = -\frac{1}{2}, \frac{1}{2}$ and $b^\dagger_\mu$ with $\mu = -\frac{5}{2}, -\frac{3}{2}, \ldots, \frac{5}{2}$ create a fermion in the $j^\pi = \frac{1}{2}^+$ and $j^\pi = \frac{5}{2}^+$ orbital, respectively. The LO Hamiltonian that governs the interactions between the fermion degrees of freedom and the quadrupole bosons is

$$H_{\rm abd} = -S(\hat{n}_a + \hat{n}_b) + \omega_1 \hat{N} + \omega_b \hat{n}_b + g_{da}\hat{\mathbf{J}}\cdot\hat{\mathbf{j}}_a + g_{db}\hat{\mathbf{J}}\cdot\hat{\mathbf{j}}_b + \omega_{2a}\hat{N}\hat{n}_a + \omega_{2b}\hat{N}\hat{n}_b. \quad (61)$$

TABLE XV. Reduced transition probabilities for phonon-annihilating $M1$ transitions in ^{103}Rh and ^{109}Ag in Weisskopf units. The uncertainty was quantified from 68% DOB intervals.

Nucleus	$I^\pi_i \to I^\pi_f$	$B(M1)_{\rm expt}$	$B(M1)_{\rm EFT}$
^{103}Rh	$\frac{3}{2}^-_1 \to \frac{1}{2}^-_1$	0.12(1)	0.10(2)
^{103}Rh	$\frac{1}{2}^-_2 \to \frac{3}{2}^-_1$		0.08(8)
^{103}Rh	$\frac{3}{2}^-_2 \to \frac{3}{2}^-_1$		0.10(4)
^{103}Rh	$\frac{3}{2}^-_2 \to \frac{5}{2}^-_1$		0.03(4)
^{103}Rh	$\frac{5}{2}^-_2 \to \frac{3}{2}^-_1$	0.014(2)	0.018(28)
^{103}Rh	$\frac{5}{2}^-_2 \to \frac{5}{2}^-_1$	0.020(3)	0.023(28)
^{103}Rh	$\frac{7}{2}^-_1 \to \frac{5}{2}^-_1$		0.17(2)
^{109}Ag	$\frac{3}{2}^-_1 \to \frac{1}{2}^-_1$	0.117(15)	0.122(27)
^{109}Ag	$\frac{1}{2}^-_2 \to \frac{3}{2}^-_1$		0.10(11)
^{109}Ag	$\frac{3}{2}^-_2 \to \frac{3}{2}^-_1$	0.16(7)	0.07(5)
^{109}Ag	$\frac{3}{2}^-_2 \to \frac{5}{2}^-_1$		0.05(5)
^{109}Ag	$\frac{5}{2}^-_2 \to \frac{3}{2}^-_1$	0.036(16)	0.033(36)
^{109}Ag	$\frac{5}{2}^-_2 \to \frac{5}{2}^-_1$	0.10(4)	0.07(4)
^{109}Ag	$\frac{7}{2}^-_1 \to \frac{5}{2}^-_1$		0.22(3)

Here, we used the operators

$$\hat{n}_a \equiv a^\dagger \cdot \tilde{a}, \quad (62)$$

$$\hat{n}_b \equiv b^\dagger \cdot \tilde{b}, \quad (63)$$

$$\hat{\mathbf{j}}_a \equiv \frac{1}{\sqrt{2}}(a^\dagger \otimes \tilde{a})^{(1)}, \quad (64)$$

$$\hat{\mathbf{j}}_b \equiv \frac{\sqrt{70}}{2}(b^\dagger \otimes \tilde{b})^{(1)}. \quad (65)$$

In the Hamiltonian (61) we omitted terms that are quartic in the boson operators. As before, S denotes the separation energy and is the largest energy scale in the Hamiltonian. The difference between the separation energies of the a and b fermions is denoted $\omega_b \approx 0.3$ MeV and is similar in size as ω_1. Interactions between the fermion orbitals are smaller corrections and omitted. The Hamiltonian (61) simply describes two fermion orbitals that interact with the quadrupole bosons but do not interact with each other. Its eigenstates are simple product states.

Within this EFT, the phonon-conserving part of the $M1$ operator has the leading terms

$$\hat{\mu} = \mu_d \hat{\mathbf{J}} + \mu_a \hat{\mathbf{j}}_a + \mu_b \hat{\mathbf{j}}_b. \quad (66)$$

Stuchbery *et al.* found the static $M1$ moments of the ground state $|(\frac{1}{2})^+_1\rangle = a^\dagger|0\rangle$ and the excited states

$$\left|\left(\tfrac{5}{2}\right)^+_1\right\rangle = b^\dagger|0\rangle \quad \text{and} \quad |I^+_f\rangle = (d^\dagger \otimes f^\dagger)^{(I)}|0\rangle, \quad (67)$$

with $f = a,b$ and $I = \frac{3}{2}, \frac{5}{2}$, of particular interest. For these states we have

$$\left\langle \left(\frac{1}{2}\right)^+_1 ||\hat{\mu}|| \left(\frac{1}{2}\right)^+_1 \right\rangle = \mu_a \sqrt{\frac{3}{2}},$$

$$\left\langle \left(\frac{5}{2}\right)^+_1 ||\hat{\mu}|| \left(\frac{5}{2}\right)^+_1 \right\rangle = \mu_b \sqrt{\frac{105}{2}},$$

$$\langle I^+_f||\hat{\mu}||I^+_f\rangle = \mu_d \Pi_i \frac{I(I+1) - F(j_f)}{2\sqrt{I(I+1)}} + \mu_f \Pi_I \frac{I(I+1) + F(j_f)}{2\sqrt{I(I+1)}}. \quad (68)$$

Here, $F(j_f) \equiv j_f(j_f+1) - 6$. The static $M1$ moments of $I^\pi = \frac{1}{2}^+, \frac{3}{2}^+, \frac{5}{2}^+$ states in odd-mass cadmium isotopes that result from the coupling of the a neutron to the even-even core are given by the expressions listed in Table X. The static $M1$ moments of state resulting from the coupling of the b neutron to the core are

$$\mu\left(\left(\frac{5}{2}\right)^+_1\right) = 5\sqrt{\frac{\pi}{3}}\mu_b,$$

$$\mu\left(\left(\frac{3}{2}\right)^+_b\right) = \frac{2}{5}\sqrt{\frac{\pi}{3}}\mu_d + \frac{13}{5}\sqrt{\frac{\pi}{3}}\mu_b,$$

$$\mu\left(\left(\frac{5}{2}\right)^+_b\right) = \frac{12}{7}\sqrt{\frac{\pi}{3}}\mu_d + \frac{23}{7}\sqrt{\frac{\pi}{3}}\mu_b. \quad (69)$$

One can adjust the LECs μ_d, μ_a, and μ_b to the static $M1$ moments of the even-even 2^+_1 and odd-mass $(\frac{1}{2})^+_1$ and $(\frac{5}{2})^+_1$

TABLE XVI. Static $M1$ moments in the ^{110}Cd $/^{111}$Cd and ^{112}Cd $/^{113}$Cd systems in units of μ_N. The static $M1$ moments labeled as $\mu_{\rm PR}$ were taken from Ref. [49] and calculated within the PR model of Ref. [74]. Values marked with an asterisk were employed to fit the LECs of the EFT. The uncertainty was quantified from 68% DOB intervals.

Nucleus	I_i^π	$\mu_{\rm PR}(I_i^\pi)$	$\mu_{\rm expt}(I_i^\pi)$	$\mu_{\rm EFT}(I_i^\pi)$
^{110}Cd	2_1^+		0.52(4)*	0.52(14)
^{110}Cd	2_2^+			0.52(28)
^{110}Cd	4_1^+			1.0(2)
^{111}Cd	$\frac{1}{2}_1^+$	−0.62	−0.59*	−0.59
^{111}Cd	$\frac{3}{2}_1^+$	0.9	0.9(6)	0.8(1)
^{111}Cd	$\frac{5}{2}_2^+$	0.8	0.5(1)	−0.07(14)
^{112}Cd	2_1^+		0.64(16)*	0.64(15)
^{112}Cd	2_2^+			0.64(30)
^{112}Cd	4_1^+			1.3(2)
^{113}Cd	$\frac{1}{2}_1^+$	−0.56	−0.62*	−0.62
^{113}Cd	$\frac{5}{2}_1^+$		−0.77*	−0.77
^{113}Cd	$\frac{3}{2}_1^+$	0.8	−0.6(10)	0.9(2)[a]
^{113}Cd				−0.3(1)[b]
^{113}Cd	$\frac{5}{2}_2^+$	0.65	0.35(10)	0.02(14)
^{113}Cd	$\frac{3}{2}_2^+$	1.2	2.1(6)	0.9(2)

[a]Value obtained by assuming the state results from the coupling of a $j^\pi = \frac{1}{2}^+$ proton to the core.
[b]Value obtained by assuming the state results from the coupling of a $j^\pi = \frac{5}{2}^+$ proton to the core.

states, respectively, and predict the static $M1$ moments of the rest of the excited states. Our results for the static $M1$ moments in the ^{110}Cd $/^{111}$Cd and ^{112}Cd $/^{113}$Cd systems are listed in Table XVI together with those of Ref. [49] calculated within the PR model of Ref. [74]. Theoretical uncertainties were quantified as $\sqrt{4\pi/3(2I+1)}C^{II}_{II10}\mu_a\delta$, where δ comes from intervals with a 68% DOB. Experimental data for the even-even nuclei were taken from Refs. [51,65], leading to values for μ_d of $0.13\mu_N$ and $0.16\mu_N$, in agreement with the naive expectation for the size of this LEC. Experimental data for states in the odd-mass nuclei were taken from Refs. [49,61,75]. Static $M1$ moments were calculated from the g factors of Ref. [49] as

$$\mu(I^\pi) = gI. \tag{70}$$

The values for μ_a of $-0.58\mu_N$ and $-0.61\mu_N$ are small but still consistent with the Schmidt value for a neutron in a $j^\pi = \frac{1}{2}^+$ orbital given by $\mu_n \approx -1.91\mu_N$. The static $M1$ moment of the $(\frac{5}{2})_1^+$ state in ^{113}Cd was assumed to be equal to that of the $(\frac{5}{2})_1^+$ state in ^{111}Cd [61]. Thus, for both cadmium systems $\mu_b \approx -0.15\mu_N$. The static $M1$ moments of the ground states in both odd-mass cadmium isotopes are well reproduced by the EFT and the PR model, although in the former case this is attributable to the fact that the static $M1$ moment of the ground state is employed to fit one of the LECs. For ^{111}Cd, the static $M1$ moment of the $(\frac{3}{2})_1^+$ state is described by both the EFT and the PR model. This is not the case for the static $M1$ moment of the $(\frac{5}{2})_2^+$ state, which is underpredicted by the EFT and overpredicted by the PR model. For ^{113}Cd, the static $M1$ moment of the $(\frac{3}{2})_1^+$ state is overpredicted by both the PR model and the EFT unless we assume that this state results from the coupling of the b neutron to the one-phonon state of the even-even core. The static $M1$ moment of the $(\frac{5}{2})_2^+$ is underpredicted by the EFT and overpredicted by the PR model, while the static $M1$ moment of the $(\frac{3}{2})_2^+$ state is underpredicted by both the EFT and the PR model. Thus the EFT and the PR model both yield a fair description of the data.

VI. SUMMARY

We have developed an EFT for the simultaneous description of spherical even-even/odd-mass systems in terms of a fermion $j = \frac{1}{2}$ degree of freedom coupled to the quadrupole degrees of freedom of the even-even core. Taking the breakdown scale around the three-phonon level in the even-even core we systematically expand energies and electromagnetic observables of states up to the two-phonon level in terms of the ratio between the corresponding energy and the breakdown scale. In the studied odd-mass isotopes of rhodium and silver, predictions for energy spectra and electromagnetic moments and transitions strengths are consistent with experimental data within the theoretical uncertainties quantified via Bayesian methods. The static $E2$ moments of excited states and phonon-conserving $E2$ transition strengths in the even-even and odd-mass nuclei follow the LO relations predicted by the EFT. While most of the data are consistently described for LECs of natural size, the strengths of phonon-conserving $M1$ transitions seems to be underpredicted by a factor of about two within the EFT. More experimental data on these transitions and/or data with an increased precision would be valuable to further test the EFT developed in this work.

ACKNOWLEDGMENTS

We thank N. J. Stone and L. Platter for useful discussions. This material is based on work supported by the Deutsche Forschungsgesellschaft under Grant SFB 124, and by the U.S. Department of Energy, Office of Science, Office of Nuclear Physics under Award No. DEFG02-96ER40963 (University of Tennessee) and under Contract No. DE-AC05-00OR22725 (Oak Ridge National Laboratory). This manuscript has been authored by UT-Battelle, LLC under Contract No. DE-AC05-00OR22725 with the U.S. Department of Energy. The United States Government retains and the publisher, by accepting the article for publication, acknowledges that the United States Government retains a nonexclusive, paid-up, irrevocable, world-wide license to publish or reproduce the published form of this manuscript, or allow others to do so, for United States Government purposes. The Department of Energy will provide public access to these results of federally sponsored research in accordance with the DOE Public Access Plan.

[1] A. Bohr and B. R. Mottelson, *Nuclear Structure*, Vol. II: Nuclear Deformations (W. A. Benjamin, New York, 1975).

[2] A. Bohr, The coupling of nuclear surface oscillations to the motion of individual nucleons, Dan. Mat. Fys. Medd. **26**, 14 (1952).

[3] A. Bohr and B. R. Mottelson, Collective and individual-particle aspects of nuclear structure, Dan. Mat. Fys. Medd. **27**, 16 (1953).

[4] J. M. Eisenberg and W. Greiner, *Nuclear Theory*, Vol. 1: Nuclear Models (North-Holland, Amsterdam, 1970).

[5] A. Arima and F. Iachello, Collective Nuclear States as Representations of a SU(6) Group, Phys. Rev. Lett. **35**, 1069 (1975).

[6] A. Arima and F. Iachello, New Symmetry in the *sd* Boson Model of Nuclei: The Group O(6), Phys. Rev. Lett. **40**, 385 (1978).

[7] P. O. Hess, M. Seiwert, J. Maruhn, and W. Greiner, General collective model and its application to $^{238}_{92}$U, Z. Phys. A: At. Nucl. **296**, 147 (1980).

[8] M. Matsuo, Anharmonicities of the double gamma-vibrational states in ^{168}Er, Prog. Theor. Phys. **72**, 666 (1984).

[9] D. J. Rowe and J. L. Wood, *Fundamentals of Nuclear Models: Foundational Models* (World Scientific, Singapore, 2010).

[10] A. de Shalit, Core excitations in nondeformed, odd-A, nuclei, Phys. Rev. **122**, 1530 (1961).

[11] A. Braunstein and A. De-Shalit, New evidence for core excitation in Au^{197}, Phys. Lett. **1**, 264 (1962).

[12] F. Iachello and O. Scholten, Interacting Boson-Fermion Model of Collective States in Odd-A Nuclei, Phys. Rev. Lett. **43**, 679 (1979).

[13] F. Iachello, Dynamical Supersymmetries in Nuclei, Phys. Rev. Lett. **44**, 772 (1980).

[14] J. Vervier and R. V. F. Janssens, Spinor symmetry and supersymmetry in the Ru, Rh, Pd, and Ag isotopes, Phys. Lett. B **108**, 1 (1982).

[15] J. Vervier, Experimental evidences for a finite number of bosons in nuclei at low spin, Phys. Lett. B **133**, 135 (1983).

[16] J. Vervier, Deviations from the center-of-gravity theorem, the monopole boson-Fermion interaction and the nuclear supersymmetry, Phys. Lett. B **149**, 267 (1984).

[17] P. Van Isacker, J. Jolie, K. Heyde, M. Waroquier, J. Moreau, and O. Scholten, The U(5) $\rightarrow$ O(6) transition in the U(612) supersymmetry scheme and its application to the odd-A Rh isotopes, Phys. Lett. B **149**, 26 (1984).

[18] J. Jolie, P. van Isacker, K. Heyde, J. Moreau, G. van Landeghem, M. Waroquier, and O. Scholten, Multilevel description of the Rh isotopes in the interacting boson-Fermion model, Nucl. Phys. A **438**, 15 (1985).

[19] A. Frank, P. Van Isacker, and D. D. Warner, Supersymmetry in transitional nuclei and its application to the Ru and Rh isotopes, Phys. Lett. B **197**, 474 (1987).

[20] G. J. Lampard, H. H. Bolotin, C. E. Doran, L. D. Wood, I. Morrison, and A. E. Stuchbery, Gyromagnetic ratios of excited states in ^{103}Rh, Nucl. Phys. A **496**, 589 (1989).

[21] M. Loiselet, O. Naviliat-Cuncic, and J. Vervier, Measurements of reduced $E2$ transition probabilities in the nuclei ^{102}Ru, ^{103}Rh, ^{106,108}Pd, and ^{107,109}Ag, Nucl. Phys. A **496**, 559 (1989).

[22] G. Maino, A. Ventura, A. M. Bizzeti-Sona, and P. Blasi, Interacting boson-Fermion model description of Ru and Rh isotopes, Z. Phys. A: Hadrons Nucl. **340**, 241 (1991).

[23] U. van Kolck, Effective field theory of nuclear forces, Prog. Part. Nucl. Phys. **43**, 337 (1999).

[24] P. F. Bedaque and U. van Kolck, Effective field theory for few-nucleon systems, Annu. Rev. Nucl. Part. Sci. **52**, 339 (2002).

[25] E. Epelbaum, H.-W. Hammer, and Ulf-G. Meißner, Modern theory of nuclear forces, Rev. Mod. Phys. **81**, 1773 (2009).

[26] R. Machleidt and D. R. Entem, Chiral effective field theory and nuclear forces, Phys. Rep. **503**, 1 (2011).

[27] H.-W. Hammer, A. Nogga, and A. Schwenk, Colloquium: Three-body forces: From cold atoms to nuclei, Rev. Mod. Phys. **85**, 197 (2013).

[28] C. A. Bertulani, H.-W. Hammer, and U. van Kolck, Effective field theory for halo nuclei: Shallow p-wave states, Nucl. Phys. A **712**, 37 (2002).

[29] H.-W. Hammer and D. R. Phillips, Electric properties of the beryllium-11 system in halo EFT, Nucl. Phys. A **865**, 17 (2011).

[30] E. Ryberg, C. Forssén, H.-W. Hammer, and L. Platter, Effective field theory for proton halo nuclei, Phys. Rev. C **89**, 014325 (2014).

[31] T. Papenbrock, Effective theory for deformed nuclei, Nucl. Phys. A **852**, 36 (2011).

[32] J. Zhang and T. Papenbrock, Rotational constants of multi-phonon bands in an effective theory for deformed nuclei, Phys. Rev. C **87**, 034323 (2013).

[33] T. Papenbrock and H. A. Weidenmüller, Effective field theory for finite systems with spontaneously broken symmetry, Phys. Rev. C **89**, 014334 (2014).

[34] T. Papenbrock and H. A. Weidenmüller, Effective field theory of emergent symmetry breaking in deformed atomic nuclei, J. Phys. G **42**, 105103 (2015).

[35] E. A. Coello Pérez and T. Papenbrock, Effective theory for the nonrigid rotor in an electromagnetic field: Toward accurate and precise calculations of $E2$ transitions in deformed nuclei, Phys. Rev. C **92**, 014323 (2015).

[36] E. A. Coello Pérez and T. Papenbrock, Effective field theory for nuclear vibrations with quantified uncertainties, Phys. Rev. C **92**, 064309 (2015).

[37] M. Cacciari and N. Houdeau, Meaningful characterisation of perturbative theoretical uncertainties, J. High Energy Phys. 09 (2011) 039.

[38] E. Bagnaschi, M. Cacciari, A. Guffanti, and L. Jenniches, An extensive survey of the estimation of uncertainties from missing higher orders in perturbative calculations, J. High Energy Phys. 02 (2015) 133.

[39] R. J. Furnstahl, D. R. Phillips, and S. Wesolowski, A recipe for EFT uncertainty quantification in nuclear physics, J. Phys. G **42**, 034028 (2015).

[40] R. J. Furnstahl, N. Klco, D. R. Phillips, and S. Wesolowski, Quantifying truncation errors in effective field theory, Phys. Rev. C **92**, 024005 (2015).

[41] P. Boutachkov, A. Aprahamian, Y. Sun, J. A. Sheikh, and S. Frauendorf, In-band and inter-band $B(E2)$ values within the triaxial projected shell model, Eur. Phys. J. A **15**, 455 (2002).

[42] N. Paar, D. Vretenar, E. Khan, and G. Colò, Exotic modes of excitation in atomic nuclei far from stability, Rep. Prog. Phys. **70**, 691 (2007).

[43] M. A. Caprio, P. Maris, and J. P. Vary, Emergence of rotational bands in ab initio no-core configuration interaction calculations of light nuclei, Phys. Lett. B **719**, 179 (2013).

[44] T. Dytrych, K. D. Launey, J. P. Draayer, P. Maris, J. P. Vary, E. Saule, U. Catalyurek, M. Sosonkina, D. Langr, and M. A.

Caprio, Collective Modes in Light Nuclei from First Principles, Phys. Rev. Lett. **111**, 252501 (2013).
[45] M. A. Caprio, P. Maris, J. P. Vary, and R. Smith, Collective rotation from *ab initio* theory, Int. J. Mod. Phys. E **24**, 1541002 (2015).
[46] G. R. Jansen, M. D. Schuster, A. Signoracci, G. Hagen, and P. Navrátil, Open *sd*-shell nuclei from first principles, Phys. Rev. C **94**, 011301 (2016).
[47] S. R. Stroberg, H. Hergert, J. D. Holt, S. K. Bogner, and A. Schwenk, Ground and excited states of doubly open-shell nuclei from *ab initio* valence-space Hamiltonians, Phys. Rev. C **93**, 051301 (2016).
[48] S. K. Chamoli, A. E. Stuchbery, S. Frauendorf, J. Sun, Y. Gu, R. F. Leslie, P. T. Moore, A. Wakhle, M. C. East, T. Kibédi, and A. N. Wilson, Measured g factors and the tidal-wave description of transitional nuclei near $A = 100$, Phys. Rev. C **83**, 054318 (2011).
[49] A. E. Stuchbery, S. K. Chamoli, and T. Kibédi, Particle-rotor versus particle-vibration features in g factors of ^{111}Cd and ^{113}Cd, Phys. Rev. C **93**, 031302 (2016).
[50] D. A. Varshalovich, A. N. Moskalev, and V. K. Khersonskii, *Quantum Theory of Angular Momentum*, 1st ed. (World Scientific Publishing, Singapore, 1988).
[51] D. De Frenne and E. Jacobs, Nuclear data sheets for A = 112, Nucl. Data Sheets **79**, 639 (1996).
[52] J. Blachot, Nuclea data sheets for A = 101, Nucl. Data Sheets **83**, 1 (1998).
[53] J. Blachot, Nuclear data sheets for A = 108, Nucl. Data Sheets **91**, 135 (2000).
[54] B. Singh and Z. Hu, Nuclear data sheets for A = 98, Nucl. Data Sheets **98**, 335 (2003).
[55] D. De Frenne and E. Jacobs, Nuclear data sheets for A = 105, Nucl. Data Sheets **105**, 775 (2005).
[56] J. Blachot, Nuclear data sheets for A = 109, Nucl. Data Sheets **107**, 355 (2006).
[57] J. Blachot, Nuclear data sheets for A = 104, Nucl. Data Sheets **108**, 2035 (2007).
[58] J. Blachot, Nuclear data sheets for A = 107, Nucl. Data Sheets **109**, 1383 (2008).
[59] D. De Frenne and A. Negret, Nuclear data sheets for A = 106, Nucl. Data Sheets **109**, 943 (2008).
[60] B. Singh, Nuclear data sheets for A = 100, Nucl. Data Sheets **109**, 297 (2008).
[61] J. Blachot, Nuclear data sheets for A = 111, Nucl. Data Sheets **110**, 1239 (2009).
[62] D. De Frenne, Nuclear data sheets for A = 102, Nucl. Data Sheets **110**, 1745 (2009).
[63] D. De Frenne, Nuclear data sheets for A = 103, Nucl. Data Sheets **110**, 2081 (2009).
[64] E. Browne and J. K. Tuli, Nuclear data sheets for $A = 99$, Nucl. Data Sheets **112**, 275 (2011).
[65] G. Gurdal and F. G. Kondev, Nuclear data sheets for A = 110, Nucl. Data Sheets **113**, 1315 (2012).
[66] L. E. Svensson, C. Fahlander, L. Hasselgren, A. Bäcklin, L. Westerberg, D. Cline, T. Czosnyka, C. Y. Wu, R. M. Diamond, and H. Kluge, Multiphonon vibrational states in ^{106,108}Pd, Nucl. Phys. A **584**, 547 (1995).
[67] N. J. Stone, *Table of Nuclear Magnetic Dipole and Electric Quadrupole Moments*, Tech. Rep. INDC(NDS)-0658 (International Atomic Energy Agency, Vienna, 2014).
[68] R. Higa, H.-W. Hammer, and U. van Kolck, $\alpha\alpha$ scattering in halo effective field theory, Nucl. Phys. A **809**, 171 (2008).
[69] L. Fernando, R. Higa, and G. Rupak, Leading $E1$ and $M1$ contributions to radiative neutron capture on lithium-7, Eur. Phys. J. A **48**, 1 (2012).
[70] L. Fernando, A. Vaghani, and G. Rupak, Electromagnetic form factors of one neutron halos with spin 1/2+ ground state, arXiv:1511.04054.
[71] C. Fahlander, A. Bäcklin, L. Hasselgren, A. Kavka, V. Mittal, L. E. Svensson, B. Varnestig, D. Cline, B. Kotliński, H. Grein, E. Grosse, R. Kulessa, C. Michel, W. Spreng, H. J. Wollersheim, and J. Stachel, Quadrupole collective properties of ^{114}Cd, Nucl. Phys. A **485**, 3271 (1988).
[72] P. B. Sogo and C. D. Jeffries, Nuclear magnetic moments of Cl^{36}, Rh^{103}, and W^{183}, Phys. Rev. **98**, 1316 (1955).
[73] D. C. Choudhury, Intermediate coupling calculations in the unified nuclear model, Dan. Mat. Fys. Medd. **28**, 4 (1954).
[74] P. Semmes and I. Ragnarson, The particle + triaxial rotor model: A users guide, Hands-On Nuclear Theory Workshop, Oak Ridge, Tennessee, USA (1991) (unpublished).
[75] J. Blachot, Nuclear data sheets for $A = 113$, Nucl. Data Sheets **111**, 1471 (2010).